UNIVERSIDADE FEDERAL DE SANTA CATARINA
PROGRAMA DE PÓS-GRADUAÇÃO EM CIÊNCIA E ENGENHARIA DE MATERIAIS

Christoffer Patrick Rahner

ANALYTICAL EVALUATION OF IMPACT TEST EQUIPMENTS TO SIMULATE HIGH CALIBER BALLISTIC THREATS

Florianópolis
Dezembro, 2012

UNIVERSIDADE FEDERAL DE SANTA CATARINA
PROGRAMA DE PÓS-GRADUAÇÃO EM CIÊNCIA E ENGENHARIA DE MATERIAIS

Christoffer Patrick Rahner

ANALYTICAL EVALUATION OF IMPACT TEST EQUIPMENTS TO SIMULATE HIGH CALIBER BALLISTIC THREATS

Dissertação submetida ao Programa de Pós- Graduação em Ciência e Engenharia de Materiais da Universidade Federal de Santa Catarina para a obtenção do Grau de Mestre em Ciência e Engenharia de Materiais
Orientador: Prof. Dr. Márcio Celso Fredel
Coorientador: Prof. Dr. Dachamir Hotza

Florianópolis
Dezembro, 2012

Catalogação na fonte elaborada pela biblioteca da
Universidade Federal de Santa Catarina

Rahner, Christoffer Patrick

ANALYTICAL EVALUATION OF IMPACT TEST EQUIPMENTS TOSIMULATE HIGH CALIBER BALLISTIC THREATS [dissertação] / Christoffer Patrick Rahner ; orientador, Prof. Dr. Márcio Celso Fredel ; co-orientador, Prof. Dr. Dachamir Hotza. - Florianópolis, SC, 2012.
51 p. ; 21cm

Dissertação (mestrado) - Universidade Federal de Santa Catarina, Centro Tecnológico. Programa de Pós-Graduação em Ciência e Engenharia de Materiais.

Inclui referências

1. Ciência e Engenharia de Materiais. 2. Material properties for armor applications. 3. Dynamic and highly dynamc impact tests. 4. Influence of the ratio between impact mass and velocity. 5. Light-gas gun facility to simulate level III / IV ballistic threats. I. Fredel, Prof. Dr. Márcio Celso. II. Hotza, Prof. Dr. Dachamir . III. Universidade Federal de Santa Catarina. Programa de Pós-Graduação em Ciência e Engenharia de Materiais. IV.Título.

Christoffer Patrick Rahner

ANALYTICAL EVALUATION OF IMPACT TEST EQUIPMENTS TO SIMULATE HIGH CALIBER BALLISTIC THREATS

Esta Dissertação foi julgada adequada para obtenção do Título de Mestre, e aprovada em sua forma final pelo Programa Programa de Pós-Graduação em Ciência e Engenharia de Materiais

Florianópolis, 17 de Dezembro de 2012.

_____
Prof. Dr. Antonio Pedro Novaes de Oliveira
Coordenador do Programa

_____
Prof. Dr. Márcio Celso Fredel
Universidade Federal de Santa Catarina, Orientador

_____
Prof. Dr. Dachamir Hotza
Universidade Federal de Santa Catarina, Coorientador

Banca Examinadora:

_____
Prof. Dr. Lauro Cesar Nicolazzi
Universidade Federal de Santa Catarina

_____
Prof. Dr. Orestes Estevam Alarcon
Universidade Federal de Santa Catarina

_____
Prof. Dr. Oscar Rubem Klegues Montedo
Universidade do Extremo Sul Catarinense

ABSTRACT

To properly evaluate materials for specific applications it is important to use experimental tests that match the application situation as best as possible. To be applied as impact tests there exist a variety of quasi-static tests, dynamic impact tests and highly dynamic impact tests. This work aims to show different design possibilities for impact test equipment of each type, to numerically analyze their potential and to evaluate the expected quality of the results of an application of said impact tests to ballistic threat experiments. The obtained results and conclusions from the studied literature and the conducted calculations show two answers about the material testing for impact properties. One is that the impact velocity has a significant influence on the impact force, also when considering the impact energy as constant. Therefore, it is recommendable to apply an experimental test that matches the simulated situation in impact energy and velocity. Second, the calculations have shown that it is possible to build a simple one-stage light-gas gun to achieve an exact replication of level III or level IV ballistic threats and therefore carry through precise testing, if utilizing a light-weight carrier as sabot. The usage of a sabot also provides an increased flexibility to the facility to test different bodies as impacting force on sample material.

RESUMO

Desejando-se avaliar o comportamento de materiais utilizados em aplicações específicas, torna-se necessário o uso de testes experimentais que simulem tal situação de trabalho da forma mais adequada possível. No caso específico de testes de impacto, existe uma variedade disponível, a saber, impacto quase estático, impacto de dinâmica baixa e impacto de dinâmica alta, etc. No presente trabalho deseja-se estudar diferentes configurações experimentais considerando os testes mencionados acima e avaliando-se numericamente os resultados esperados quando aplicados em testes balísticos. Os resultados obtidos a partir do estudo da literatura e dos cálculos conduzidos, mostram duas conclusões principais relacionadas aos testes de propriedades de impacto em materiais. A primeira é a velocidade de impacto tendo alta influência sobre a força de impacto, também quando a energia de impacto é considerada constante. Assim, recomenda-se a utilização de um teste experimental com parâmetros iguais a situação simulada, especificamente em energia e velocidade de impacto. A segunda é que os cálculos mostram ser possível a realização de testes precisos balísticos de nível III ou IV, utilizando-se uma estação simples de arma de gás leve (one-stage light-gas gun) com o auxílio de uma base de suporte baixo (sabot). O uso do sabot também fornece um aumento na flexibilidade da estação podendo-se utilizar projéteis com diferentes geometrias e tamanhos para as amostras de material em análise.

LIST OF FIGURES

LIST OF TABLES

TABLE OF CONTENTS

1 INTRODUCTION

The global market for personal protection systems alone is worth 300-400 million Euros per year. Everywhere in the world it is enjoying growth rates of more than 5 percent. Ballistic protection is generally used by those in the armed forces and law enforcement, and by politicians, entrepreneurs and celebrities afraid of being the target of an assassination attack. The amount of money being spent on research and development is high; every company wants to come up with the perfect ballistic protection solution. Dreams of flexible, lightweight, effective and intelligent body armor are a long way off, but hopeful approaches lie with nanotechnology. Nanocomposites offer superior protection and are incredibly light; however, they are also exceedingly expensive (Connor, 2006).

1.1 BALLISTIC PROTECTION OVERVIEW

The design and production of a ballistic protection system as a project in a given company can be viewed as a task that consists of different concerns: cost & effort, test / evaluation, product design and (raw) material(s), as drawn in Figure 1. Moreover, this Figure shows a group of means and methods that are connected to one or several of those areas. The focus of each area can be described as follows:

- Cost & effort describes the technological and financial limitations that govern the project of any given design and construction of a ballistic protection. The financial aspect covers as well the costs of the development as well as the costs of production which determines the price of the final product. The technological aspect on the other hand is defined by the availability of machines, equipment and know-how and the environment in which the product is to be developed or produced. Any company would obviously prefer to focus on production methods they already use for other production processes to achieve synergy effects and to minimize investment costs.
- Product design is constituted by any geometrical definitions such as the type of object that is to be protected; personal protection vests are rather limited in their freedom of design, as the protection vest has to follow the contours of a human body without hindering

movement or exceeding the weight that the an individual would be able to carry. Another aspect is the structure of the protective system: By forming the system in a certain way the performance might be improvable as well. For example, there has been a long discussion over the advantages and disadvantages of replacing monolithic plates by multi-layered plates either with or without spacing (Zhou and Stronge, 2008) or the effect on the ballistic performance of rubber, Teflon and aluminum foam used as interlayer material of composite armor systems (Tasdemirci et al.,2012). Another approach to optimize the layered system is from Ong et al. (2011): They developed a design of composite personnel armor by optimizing consisting of four layers, wherein each layer plays a specified role during projectile impact. A very hard 1st layer is applied to deform and fracture the projectile, an orthotropic 2nd layer to slow down the shock wave propagation in the through thickness direction, while permitting fast propagation in the transverse directions, the shock wave energy is absorbed by a 3rd porous layer through PV-work, and a 4th layer to provide confinement for the porous medium.

- The area (raw) material(s) describes the part of ballistic protection engineering that examines existing materials to obtain their relevant properties, improve these properties by adding or removing additives or to develop new material composites. This includes for example adding a new combination of fibers and matrix material, or an entirely new composite by combining materials with a different method that changes the composites properties. Sometimes different approaches can even lead to the combination of materials previously thought to be impossible to combine.
- The fourth area is Test & Evaluation. To evaluate a planned ballistic protection systems' potential, to control produced systems and to test new approaches, it is necessary to design facilities which are able to simulate the situations and obstacles the product will

have to withstand to obtain reasonable results. The experimental simulation of possible strain or stress situations of a products application require evaluation that the product can withstand these strains/stresses and fulfill the task for which it is designed. Small changes in the type of strain or stress can differ highly in the outcome of the situation. Therefore, it is inevitable to either design experimental facilities that describe the situation at hand as exact as possible, or prove experimentally that it is possible to transfer the acquired data from an experiment which differs somewhat from the situation in question to the desired result is possible by for example by an analytical transition.

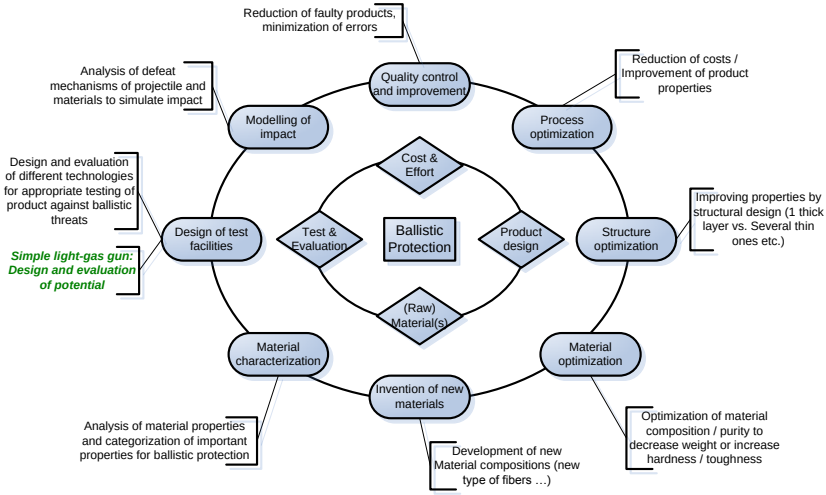

Figure 1: Ballistic protection overview

Each of these four areas interacts with the others. For example, the optimization of processes or structures is an important tool to reduce costs and efforts as well as for the design of a product. The modeling of an impact situation is as important the testing department as it is a tool to maintain low costs by ensuring that the planned system will deliver satisfying results already in the prototype phase.

1.2 AIM OF WORK AND JUSTIFICATION

The knowledge of material properties involved in impact situations is critical in different technological areas in order to guarantee safe operations. For this specific equipment tools are needed. In this context, the aim of this work is to evaluate the possibilities and limitations of constructing a simple one-stage light-gas gun to test materials for impact resistance. For this, the achievable muzzle velocities with different driving gas, pressure reservoirs and barrel lengths utilizing a 7.62 mm projectile with a mass of 9.6 g (Level III as described below) will be calculated and analyzed.

2 OVERVIEW ON PROTECTIVE SYSTEMS

2.1 CERAMICS AND THEIR APPLICATION AS ARMOR

The processing of ceramics is one of the oldest industries in the history of mankind. Already our nomadic ancestors discovered about 24000 B.C. that clay can be given form by mixing it first with water and then firing. The first ceramic objects to be processed were figurines of animals and humans. The first tiles were produced at around 14000 B.C. in Mesopotamia and India, after humans had settled down. The earliest clay bricks and functionary storage devices date from 9000 to 10000 B.C. Since then the technology of processing and designing ceramic materials has far evolved, presenting today a huge variety of different materials for different applications. Generally ceramics present a relative high resistance together with a relatively low density (Sniles, 2009).

Ceramic materials present a heterogenic distribution of flaws due to the nature of the powder that are stay through all processing and densifications. Typically flaws are caused by unintended inclusions of organic or inorganic material in the raw material. In ductile materials, like metals, these types of flaws do not lead to critical failure since they exhibit deformation mechanisms that absorb energy at breaking points. At room temperature, both crystalline and noncrystalline ceramics almost always fracture before any plastic deformation can occur in response to an applied tensile load (Callister Jr., 2007).

The brittle fracture process consists of the formation and propagation of cracks through the cross section of material in a direction perpendicular to the applied load. Crack growth in crystalline ceramics may be either transgranular (i.e., through the grains) or intergranular (i.e., along grain boundaries); for transgranular fracture, cracks propagate along specific crystallographic (or cleavage) planes, planes of high atomic density (Callister Jr., 2007). Figure 2 shows the comparison of these two types of fractures for a pure ceramic material (alumina) and alumina composites, studied by different authors. As can be seen, fracture on monophase alumina had the tendency to crack intergranular while the composites tend to transgranular fracture behavior.

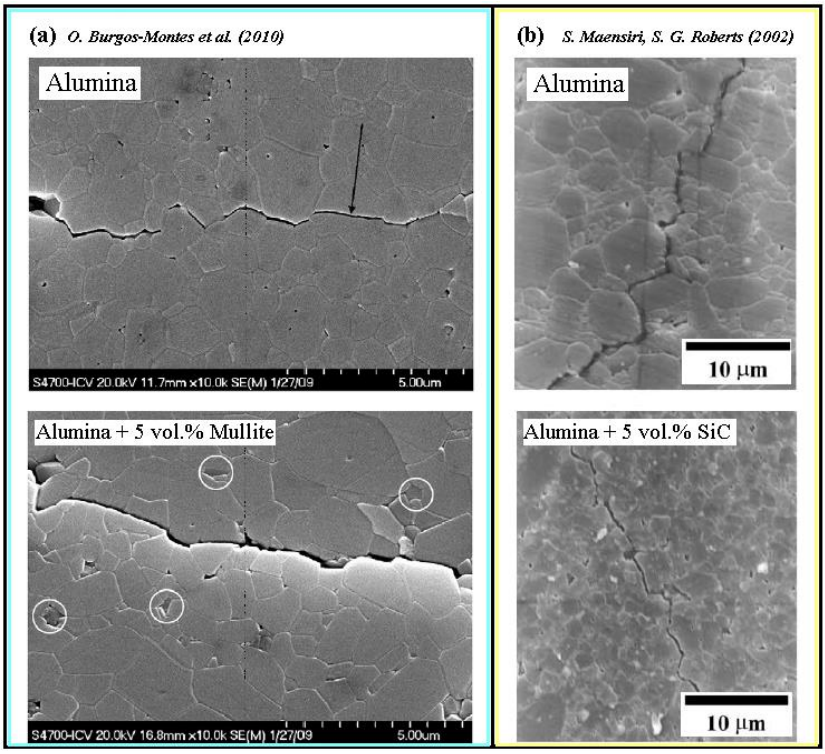

Figure 2: Comparison of fracture behavior in: (a) pure alumina (Burgos-Montes et al., 2010); and (b) alumina composites (Maensiri and Roberts, 2002)

The measured fracture strengths of ceramic materials are substantially lower than predicted by theory from interatomic bonding forces. This may be explained by very small and omnipresent flaws in the material that serve as stress raisers – points at which the magnitude of an applied tensile stress is amplified. The degree of stress amplification depends on crack length and tip radius of curvature being greatest for long and pointed flaws. These stress raisers may be minute surface or interior cracks (microcracks), internal pores, and grain corners, which are virtually impossible to eliminate or control. For example, even moisture and contaminants in the atmosphere can introduce surface cracks in freshly drawn glass fibers; these cracks deleteriously affect the strength. A stress concentration at a flaw tip can

cause a crack to form, which may propagate until the eventual failure (Callister Jr., 2007).

The evolution of armored vehicles and combat armors goes together with the development of ammunition. To maintain agility in combat it is important to use materials or composites that provide a good protection as characterized by elasticity modulus, hardness and toughness but as well a low weight. Nowadays the best solutions include composites made with layers of ceramics (Al_2O_3, SiC, B_4C) in combination with polymers (aramid fibers or glass fibers). In general, employed solutions present a single ceramic plate which once hit by the impact of a projectile will suffer catastrophic failure and break therefore losing the initial protection ability. The performance of the composite can be improved by forming it as a construction with several small plates of high performance ceramic. In this way the performance can be improved if the surface of the first plate has a determined angle in relationship to the path of impact of the projectile. Table 1 gives a short overview over common ceramic materials for armor applications (Karandikar et al., 2009).

Table 1: Summary of properties of ceramics for personnel armor application (adapted) (Karandikar et al., 2009).

Material	Designation	Density (g/cm^3)	Grain Size (µm)	Young's Modulus (GPa)	Flexural Strength (MPa)	Fracture Toughness ($MPa.m^{1/2}$)	For Fracture Mode	Hardness (kg/mm^2)	HK 2 kg (kg/mm^2)	Areal Density lb/ft²*
Al_2O_3	CAP-3	3.90	-	370	379	4-5	-	1440 (HK 1 kg)	1292	20.2
B_4C	Ceralloy-546 4E	2.50	10-15	460	410	2.5	transgranular	3200 (HV 0.3 kg)	2066	13.0
	Norbide	2.51	10-15	440	425	3.1	transgranular	2800 (HK 0.1 kg)	1997	13.0
SiC	SiC-N	3.22	2-5	453	486	4.0	intergranular, transgranular	-	1905	16.7
	Ceralloy 146-3E	3.20	-	450	634	4.3	-	2300 (HV 0.3 kg)	-	16.6
	Hexoloy	3.13	3-50	410	380	4.6	transgranular	2800 (HK 0.1 kg)	1924	16.2
	Purebide 5000	3.10	3-50	420	455	-	transgranular	-	1922	16.1
	SC-DS	3.15	3-50	410	480	3-4	-	2800 (HK 1kg)	-	16.4
	MCT SSS	3.12	3-50	424	351	4.0	transgranular	-	1969	16.2
	MCT LPS	3.24	1-3	425	372	5.7	intergranular, transgranular	-	1873	16.8
	Ekasic-T	3.25	1-3	453	612	6.4	intergranular, transgranular	-	1928	16.8
SiC (RB**)	SSC-702	3.02	45	359	260	4.0	transgranular	1757 (HK 0.5 kg)	-	15.7
	SSC-802	3.03	45	380	260	4.0	transgranular	-	1332	15.7
	SSC-902	3.12	45	407	260	4.0	transgranular	-	1536	16.2
SiC/B_4C (RB**)	RBBC-751	2.56	45	390	271	5.0	transgranular + Ductile Si	-	1626	13.3
TiB_2	Ceralloy 225	4.50	-	540	265	5.5	-	-	1849	23.4

Sources: CAP-3, SC DS: Coors Tek; Ceralloy, Ekasic-T: Ceradyne; Norbide, Hexoloy; Saint Gobain; Purbide: Morgan AM&T; SiC-N: Cercom (BAE); SSC, RBBC, BSC, SSS and LPS - M Cubed Technologies (MCT). Properties for other manufacture's materials are from their respective websites except for 2 kg Knoop herdness, grain size and fracture mode.

* Areal density: mass of 12 x 12 x 1 inch panel in pounds. ** RB: reaction bonded

2.2 ARMOR MATERIALS AND SYSTEMS

Protection in battle or simply in dangerous times has always been on man's mind. Over the centuries, several countries over the globe developed protection clothing for use during combat. Hard linen was used in up to 14 layers by Mycenaeans already in the sixteenth century B.C., while Persians and Greeks applied the same technique around the fifth century B.C. Until the nineteenth century Micronesian inhabitants

of the Gilbert and Ellice Islands used woven coconut palm fiber. In other cultures armor was made from the hides of animals: already in the eleventh century B.C. the Chinese wore rhinoceros skin in five to seven layers, and the Shoshone Indians of North America glued or sewn together several layers of hide to produce protective clothing. Armor made by quilting was set to use by tribes in Central America before the Spanish conquests, in England around the seventeenth century, and in India until the nineteenth century. Figure 3 shows the traditional quilted armor of the Hausa, an African tribe from western and central Africa, mainly from Nigeria.

Figure 3: Hausa (African tribe) armed horsemen in quilted armor at Independence Day celebration (NMAfA, 2012)

Metal armor consisted usually of linked rings or wires of iron, steel, or brass. The Roman Empire outfitted its soldiers with mail shirts, which remained state of the art in Europe until the fourteenth century. Mail armors were also developed in Japan, India, Persia, Sudan, and Nigeria. In the eastern Hemisphere from about 1600 B.C. until modern times overlapping scales of metal, horn, bone, leather, or from an animal were used to produce a (scale) armor. Sometimes, as in China, the scales were sewn into pockets as an inlet in the way ceramic inlets are used for modern body armor.

Figure 4: Brigandine armor (remodeled) (Nadler, 2006)

Another armor that used a sort of inlets was the Brigandine armor, displayed as Figure 4. Quilted jackets with small overlapping rectangular iron or steel plates riveted onto leather strip, making it light, flexible jacket. Earlier sets of plates from twelfth-century Europe were heavier and stiffer. They were followed up by the familiar full-plate suit of armor of knights of the 1500s and 1600s. The brigandine armor, as used by the Chinese and Koreans armor around A.D. 700 and during the fourteenth century in Europe, is considered by many to be the archetype of modern ballistic protection vests.

With the introduction of firearms, armor crafts workers augmented the torso cover, using thicker steel plates and a second heavy plate, to be able to withstand a gunshot. In practice, those heavy armors were usually discarded wherever firearms came into military use.

Research continued to find effective armor against gunfire, especially during the American civil war as well as World War I and II. One example can be seen in Figure 5, demonstrated by the police force of Berlin in 1931. This type of vest consisted of ballistic nylon

reinforced by plates of fiber-glass, steel, ceramic, titanium, Doron, or composites of ceramic and fiberglass.

Figure 5: Early protective vest, demonstration by Berlin police force (Bundesarchiv, 1931)

Ballistic nylon remained the standard material used until the 1970s. In 1965, a DuPont chemist named Stephanie Kwolek developed poly-paraphenylene terephthalamide, or Kevlar. Kwolek designed it originally to use it in tires, ropes, gaskets, and various parts for planes and boats. In 1971, Lester Shubin of the National Institute of Law Enforcement and Criminal Justice set it to use replacing the ballistic nylon in bulletproof vests, and it has been the material of choice ever since. In 1989, the Allied Signal Company developed a rival for Kevlar, naming it Spectra. Originally designed to produce sails, it is now possible to create lighter, yet stronger, nonwoven material with polyethylene fibers to be applied in bulletproof vests along-side the traditional Kevlar. Recently, Magellan Systems International in partnership with DuPont Advanced Fiber Systems developed a new fiber with high potential for use in armor systems for personnel and vehicles, flame and thermal protection, as well as in high performance

structural composites. Based on test results carried out by U.S. military, it is estimated that fragmentation protective armor systems based on M 5 will reduce the areal density of the ballistic component of these systems by approximately 40-60% in comparison to Kevlar KM2® fabric at the same level of protection (BodyArmorNews, 2012).

Potential army applications of the fiber include fragmentation vests and helmets, composites for use in conjunction with ceramic materials for small arms protection and structural composites for vehicles and aircraft. Still, these vests offer only protection against handguns. In order to obtain protection against rifles or high caliber handguns, the vest is reinforced with inlet of metal or ceramic. Those inlets require a certain thickness depending on the level of protection, making the vest heavier and more inflexible again. Therefore, inventing new methods of improving the level of protection without increasing the overall weight remains to be in focus for researchers and industry. Approaches include composite materials and fiber-enforced ceramics.

A similar development can be found in the protection of vehicles. To find a suitable protection for passengers, cargo and/or sensitive parts of the vehicle like tires or the engine a balance between protection level and weight is needed. This applies to military armored transport vehicles over civilian armored transport such as money transport and armored personal cars as well. For the latter, the vehicle of choice is usually a luxury sedan, reinforced with armor plating. Mercedes has been building "special protection" cars since 1928. One of its earliest models, a 1935 behemoth, the Grand Mercedes, was better known as Emperor Hirohito's limousine, shown in Figure 6.

Figure 6: Mercedes 770 Pullman Limousine was owned by Japan's Emperor Hirohito, Mercedes-Benz museum (Motortrend, 2006)

Today, armored cars are a booming market. According to the Brazilian Association of Armor (Associação Brasileira de Blindagens), the number of protected vehicles increased between 1999 and 2009 by 177 %, while the number of cars only increased by 84 %. Many people feel afraid to drive cars unprotected, as well as academics in big cities such as São Paulo as well as soy planters in the interior of Rio Grande do Sul. This development is supported by technological improvements to offer cheaper solutions and also solutions with less weight to also fit smaller cars. As an average, to armor a car to NIJ Level IIIA, the level of choice for most customers of one the several companies that offer armoring services, adds a weight of 200 kg and costs around 28,000 USD if done by a company certified by the Police (Concept Blindagens, 2012).

3 STATE OF ART

3.1 MATERIAL PROPERTIES FOR ARMOR APPLICATIONS

Several criteria are to be taken into account when choosing materials for ballistic protection application. The level of protection, meaning therefore the characteristics of the ballistic threat that the protective system is supposed to withstand, price as economic limitation as well as physical constraints such as weight and volume are the key determinants. Since some characteristics, e.g. weight and level of protection, are somewhat of contrary nature, there is no best solution or best overall material. If a higher flexibility and mobility of a person wearing body armor is required, one option might be to reduce weight by reducing the amount of material used – which would obviously reduce the protective abilities of the armor system.

Table 2: Material properties and their role in ballistic performance (adapted) (Karandikar et al., 2009)

Property	**Role / Effect in ballistic performance**
Microstructure Grain size Minor phases Phase transformation or Amorphization (stress induced) Porosity	Affects all properties listed in the left-hand column below
Density	Weight of the armor system
Hardness	Damage to the projectile
Elastic Modulus	Stress wave propagation
Strength	Multi hit resistence
Fracture Toughness	Multi hit resistence, field durability
Fracture Mode (Inter vs.Trans Granular)	Energy absorption

A variety of ceramics are available for use in personnel armor applications. The key material properties that may be used to aid in the selection of ceramics are density, hardness, fracture mode, toughness and the microstructure regarding grain size, amount of minor phase, and phase stability. More recently discovered phenomena of pressure-induced amorphization or phase transformation in some materials are becoming increasingly more critical when designing armor systems to defend against high tenacity projectiles (Karandikar et al., 2009).
Table 2 gives a brief overview on the most important material properties for armor applications. Besides the material density and weight, especially hardness and fracture toughness is of higher importance.

Generally, a higher hardness than that of the projectile is necessary in order to successfully defeat the threat. High fracture toughness might allow the system to withstand multiple hits. Unfortunately, those properties tend to follow an inverse relationship in most materials. This relationship is displayed in Figure 7 for some materials as hardness is platted as a function of their toughness. The lines in the plot show the hardness of some representative projectile materials as a comparison. The Al/SiC metal matrix composites (MMCs) have low hardness but very high fracture toughness. Those materials could be useful as a component of armor systems designed to protect against low hardness threats. To defeat tool steel and WC bullets it is necessary to compose the armor system with higher hardness ceramics (Karandikar et al., 2009).

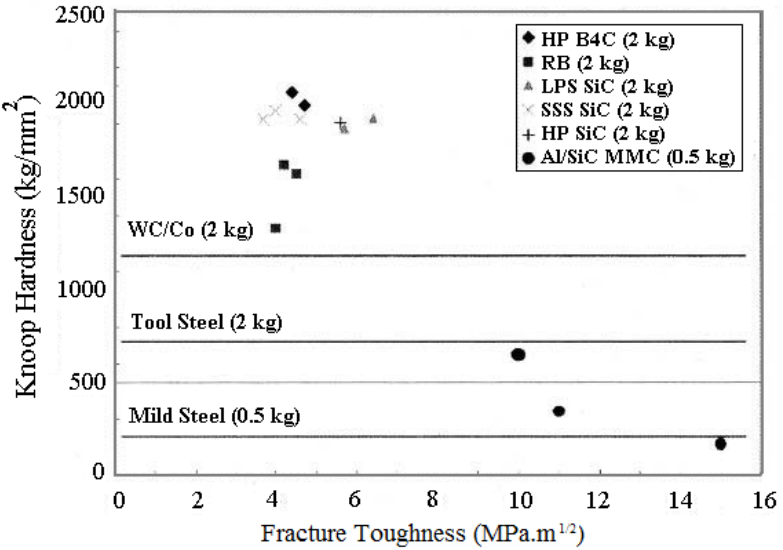

Figure 7 Hardness against fracture toughness for different ceramic materials (Karandikar et al., 2009)

The elastic modulus is also important to influence the shockwave propagation, especially for body armor to prevent "blunt traumas". Minor phases present in the ceramic have a great influence on the elastic modulus and also on the ballistic impact resistance. Armor ceramic materials contain a variety of minor phases due to the nature of their respective manufacturing processes. Figure 8 displays a graph of elastic

modulus as a function of minor phase content. In general, the presence of such minor phases leads to a reduction of the elastic modulus, depending on the type of minor phase with porosity causing the biggest reduction. Similar effects on other properties critical to ballistic performance can be expected.

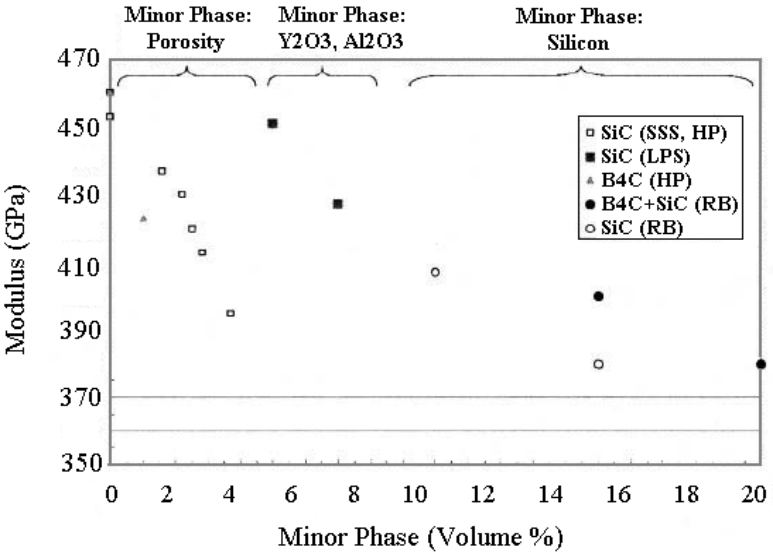

Figure 8: Minor phases effect on elastic modulus of ceramic materials (Karandikar et al., 2009)

3.2 BALLISTIC THREAT CATEGORIZATION

Ballistic threats are categorized by different organizations in different levels depending on the utilized firearm and the type of ammunition. The most common categorization is by the United States Department of Justice's National Institute of Justice (NIJ). Table 3 shows the physical data for the projectiles for each level of protection that are used at the test of new protection materials. A full metal jacket (FMJ) is a bullet consisting of a soft core encased in a shell of harder metal. This type exists with different shaped projectiles, e.g., round-nosed (RN) and flat-nosed (FN). A jacketed soft-point bullet (JSP) is a lead expanding bullet with a jacket that is left open at the tip, exposing some of the lead inside and is thus an example of a semi-jacketed round. A semi-jacketed hollow-point bullet (SJHP) is an expanding bullet as

well that has a pit or hollowed out shape in its tip to expand upon entering a target in order to decrease penetration and disrupt more tissue as it travels through the target. The materials of the projectiles of threat levels IIA, II and IIIA are lead as core and a copper alloy of approximately 90% copper and 10% zinc as coating; threat level III uses steel as coating. The level IV projectile is a special military armor-piercing round with a copper alloy coating and a steel penetrator core (NIJ 2006).

Table 3: Mass, velocity and kinetic energy of NIJ test projectiles (NIJ, 2006).

NIJ BODY ARMOR CLASSIFICATION / KINETIC ENERGY				
Type	**Test calibre**	**Mass [g]**	**Velocity [m/s]**	**Energy [J]**
Type IIA	9 mm FMJ RN	8	373	557
	.40 S&W FMJ	11.7	352	725
Type II	9 mm FMJ RN	8	398	634
	.357 Magnum JSP	10.2	436	969
Type IIIA	.357 SIG FMJ FN	8.1	448	813
	.44 Magnum SJHP	15.6	436	1483
Type III	7.62 mm FMJ (M80)	9.6	847	3444
Type IV	.30 AP (M2 AP)	10.8	878	4163

Soft armor, textile based systems using high performance fibers, are able to defeat low level threats (NIJ Level IIIA or less, see Table 3). Hard armors are reinforced by metal or ceramic inlets to deal with higher level threats (NIJ Level III+); low density ceramics (with density 2.5-4.0 g/cm³) provide higher hardness while weighing less than half at the same thickness in comparison with steel (density 7.8 g/cm³).

Today's typical routine vests as used by patrol officers are such soft vests which can provide protection to most low and medium energy handgun rounds. Hard body armor designed to defeat rifle fire are usually reserved for use in special situations where it is worn externally, as opposed to the usually concealed soft body armors, for short periods of time when confronted with higher level threats, due to its weight and bulkiness.

As for personal armors, the protection systems for vehicles depends on the type of vehicle. An armored personal car will usually be equipped with protective systems sufficient to defeat level IIIA threats, therefore soft inlets integrated into the car walls usually prove sufficient. For the average car this mass addition will already be a limit to the

performance of the car. Specially manufactured personal cars or transports or military vehicles on the other hand can be equipped with protection against more powerful threats utilizing hard armor inlets as well.

3.3 IMPACT MECHANICS AND DEFEATING MECHANISMS

Zhou and Stronge (2006) investigated different models to calculate the result of an impact on a sandwich structure. Along other variables they also paid attention to the influence of velocity on the impact force. Their work suggests that the validity of the used models strongly depends on the ratio between the mass of the projectile and the effective mass of the target object, in that case a light-weight sandwich plate, if the damage behavior can best be described using quasi-static model or a dynamic model.

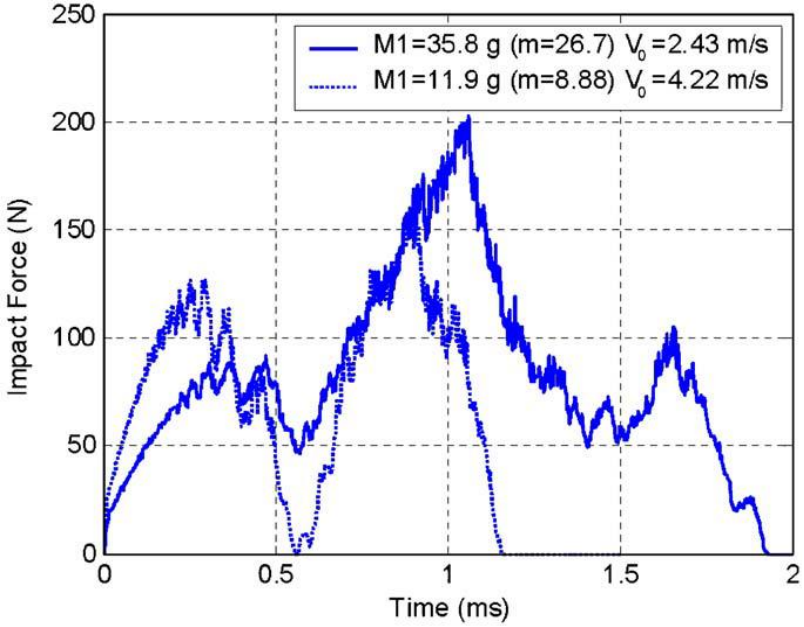

Figure 9: Impact force for two projectiles with initial kinetic energy of 110 mJ and different velocities (Zhou and Stronge, 2006)

Figure 9 shows a part of these results; two spherical projectiles were launched on a sandwich panel. Both have an initial kinetic energy

of 110 mJ, but one is with 35.8 g heavier and 2.43 m/s slower than the other one with 11.9 g and 4.22 m/s. The graph shows that the heavier projectile generates a larger impact force (Zhou and Stronge, 2006).

3.3.1.1 Ballistic impact on a soft armor system

Upon striking a soft body armor, a bullet is caught in a web of very strong fibers, if the armor system is strong enough to defeat the ballistic threat in question. The energy of the impact is absorbed by the fibers, which causes the bullet to deform. Each successive layer absorbs a part of the energy until the projectile is stopped. This cooperation of the fibers work both in each single layer as well as with the successive layers of material, a large part of the protective vest is involved in stopping the bullet from penetrating. This also helps in preventing the impact to cause "blunt trauma" or non-penetrating injuries to internal organs (BodyArmorNews.com).

3.3.1.2 Ballistic impact on hard armor system

As laid out before, common hard armor systems include a ceramic tile backed by a fiber reinforced polymer matrix composite. The processes occurring upon impact of a projectile is shown in Figure 10.

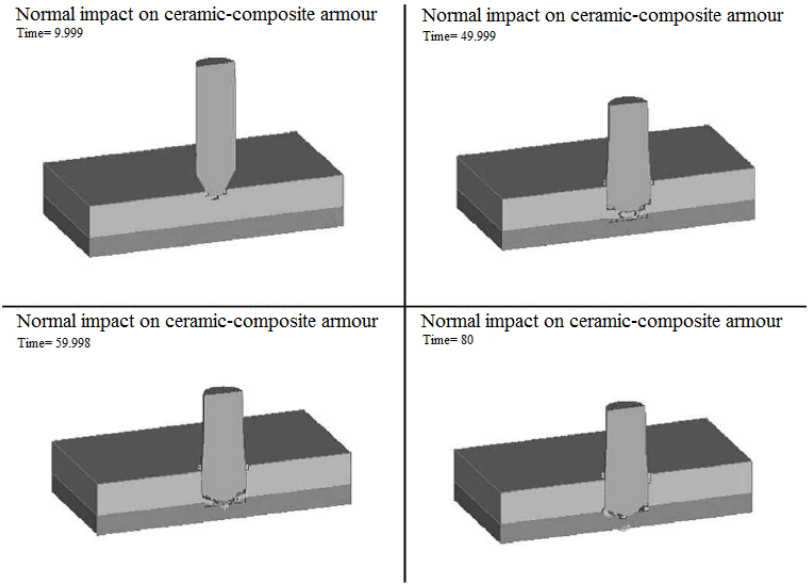

Figure 10: Impact on Ceramic-Composite Armor (Fawaz, 2004)

Upon impact of the projectile upon the strike face (the ceramic), the kinetic energy generates a shock wave in the ceramic leading to tensile, compressive and shear stresses in different magnitude depending on the threat. Cracks are generated in the ceramic and the ceramic imparts stress back on the projectile, whereby the projectile is deformed, shattered or eroded.

The projectile or fragments might go on to penetrate the ceramic, depending on the force of the threat. The fragments (projectile and ceramic) are stopped by the composite backing, if the protective system is able to defeat the threat. Otherwise the projectile or some fragments travel through the system and hit the wearer. A residual deformation might be created on the back side of the armor system, transferring the momentum to the wearer's body, possibly leading to “blunt traumas”.

To successfully defeat a projectile, it must be significantly deformed it or broken it into pieces and thereby the kinetic energy sufficiently reduced so the ceramic or the backing can stop it without causing major back face deformation or even penetration. The ceramic must be sufficiently robust to make the projectile spend sufficient time interacting with the surface of the ceramic to damage the projectile is sufficiently so as to preclude further penetration of the armor system.

3.3.1.3 Destructive defeat of a projectile

As stated before, hard body armors consist of a hard protection inlet, usually ceramic, and a ductile backing, which is made either of metal or of polymer like Kevlar. The task for the hard inlet is to take the initial impact and to destroy the head of the colliding body. If strong enough, the armor system is capable of defeating velocity projectiles on the surface of the ceramic, a so-called interface defeat. This means that the projectile material is forced to flow radially outwards on the surface of the ceramic without penetrating significantly. This capability would not only defeat the ballistic threat but also protect ceramic materials from damage and thus keeping the protective system intact to withstand another threat. Lundberg et al. developed a model to simulate this situation. They treated the projectile as a stationary jet with a certain compressibility and strength, while they considered the impact surface to be flat, rigid and friction-free. Essentially, their model considered the loading to be quasi-static, which is not true initially when the projectile hits the target. Therefore, additionally some kind of attenuating device had to be used to achieve nearly quasi-static experimental results (Lundeberg et al., 2000).

Gonçalves et al. (2004) separate the process of defeating a ballistic impact on an armor system into two stages. In the first stage the projectile impacts on the hard inlet resulting in a destruction of the head of the projectile and in stress waves in the hard inlet created by the initial impact. In this initial stage the major part of the projectile's impact energy is absorbed. In the second stage the remaining parts of the projectile proceed to penetrate the armor system, while the backing material conducts the absorption of the residual impact energy until the fragments cease to move. This penetration leads to a deformation of the ductile backing material. During the penetration, the interface of the projectile and the armor system can be considered as a moving part into the armor system. However, it is moving with a slower velocity than the rear end of the projectile, thus leading to erosion of the projectile. During this process the interface experiences acceleration while the projectile is decelerated until they travel with the same speed until the kinetic energy is entirely absorbed and the projectile is stopped. Figure 11 shows the projectile and interface velocity during this stage as a function of time.

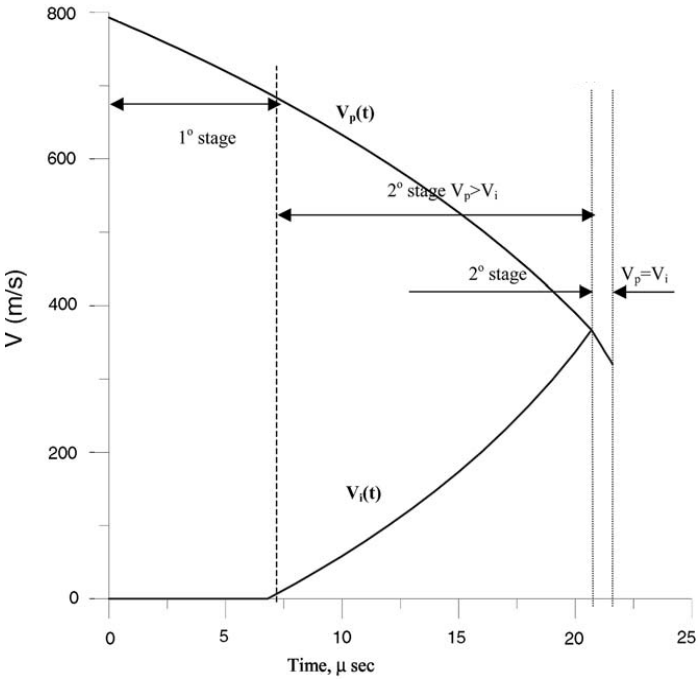

Figure 11: Projectile velocity vp and interface velocity vi as a function of time (Gonçalves et al., 2004)

Table 4 shows the result of a numerical simulation: the loss of velocity, the erosion of the projectile and the absorbed energy. In this case the process is divided in three stages. The first stage describes the impact of the projectile on the front armor material, destroying the head of the projectile until commencement of the actual penetration. In this stage 19.18% of the initial mass is removed, the projectile gets slowed down 10.62% of its impact velocity and 35.73% of the energy gets absorbed. The second stage consists of the beginning of the penetration until the projectile and the interface velocity are equal. During this part, the main part of the kinetic energy is absorbed (50.32%), and a good part of the projectile is eroded (40.77%). Further, the velocity is reduced by 30.27%. During the last stage, the remaining projectile fragments and the interface continue to travel into the armor system without further eroding, but although they are moving at 59.10% of the initial velocity, only the remaining 13.93% of energy have to be absorbed until the threat is completely defeated.

Table 4: Absorbed energy during impact defeat (Neckel, 2012)

Stage	Loss of velocity (%)	Erosion (%)	Absorbed energy (%)
1°	10.77%	19.18%	35.65%
2°	50.67%	49.27%	59.66%
3°	38.57%	-------	4.69%

4 METHODS AND MATERIALS

4.1 IMPACT TESTS

Impact tests are a common mean to simulate materials and structures under the influence of an impact situation such as collision of cars and ships, impact of small stones on the windshield of a moving vehicle or ballistic threats. They can be differenced in various types. In this work they are categorized as quasi-static, dynamic impact and highly dynamic impact tests. Each type of tests aims to evaluate objects for their behavior in different situations depending on impacting energy, velocity, and hardness as discussed below.

4.1.1 Quasi-static tests

Quasi-static experiments are no impact tests; they provide material properties by obtaining resistances and strengths. Usually this is achieved by applying a load on samples. Examples for such tests are the 3-point and the 4-point bending tests to obtain the flexural strength, as displayed in Figure 12.

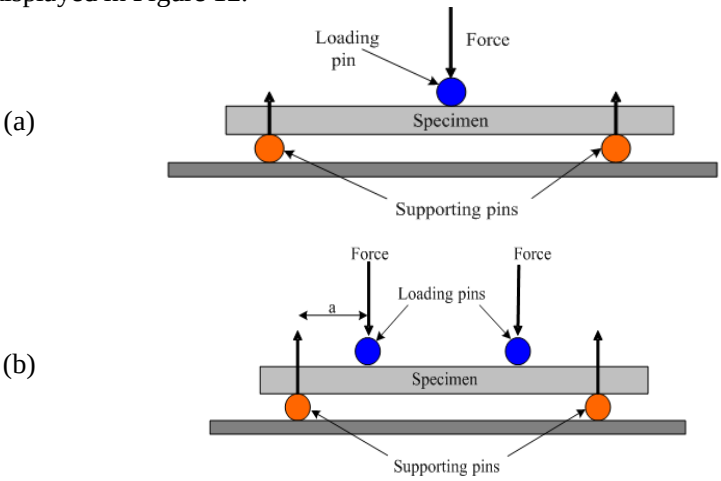

Figure 12: Schematic drawing of (a) 3-point and (b) 4-point flexure tests (SubsTech, 2012)

The flexural strength can be obtained by calculation using the Equations 1 and 2, respectively for 3-point or 4-point bending test of a rectangular shaped sample:

$$\sigma = \frac{3LF}{2bd^2} \quad (1)$$

$$\sigma = \frac{3Fa}{bd^2} \quad (2)$$

where L is the specimen length, F is the total force applied to the sample by the loading pin(s); b is the specimen width; d is the specimen thickness of the; and a is the distance between the supporting and loading pins (SubsTech, 2012).

Zhou and Stronge (2006) showed that with a certain mass ratio m_r between colliding projectile and target sample it is possible to simulate an impact situation as a quasi-static test. They regarded the mass ratio $m_r = 8$ as the minimum for a quasi static model. That means that the projectile has mass 8 times higher than that of the sample. The expected impact situation in this work on the other hand assumes the mass of the projectile to be much lower than that of the target, since an armor system consisting of a ceramic/polymer composition will have a few kg of mass as opposed to the ~10 g mass of a level III / level IV projectile.

4.1.2 Dynamic impact tests

Dynamic impact tests are conducted by experimental facilities that consist of one moving or impacting part that will hit upon a target sample with a determined kinetic energy built from a certain mass and a certain impact velocity. Common tests in this group are the Charpy impact test and the free-fall-tower impact test, as described in the following sections.

4.1.2.1 Charpy impact test

The Charpy impact test is a standardized tool to study temperature-dependent ductile-brittle transition. It measures the amount of energy absorbed by a given material during fracture which determines that notch toughness. As an easy test to prepare and carry out

it is widely applied in industry, providing a quick and cheap way to obtain results. On the downside, some of its results are only comparative (Meyers and Chawla, 1998).

The Charpy impact test equipment consists of a pendulum hammer of known mass and length which is hold at a predetermined height and, upon release, impacts a notched specimen of material. The difference in the height of the hammer before and after the fracture displays the energy absorbed by the fracture event. Variables like specimen size, shape as well as notch geometry and depth influence the test results (Mills, 1976; Kurishita et al., 1993; Callister Jr., 2007)

4.1.2.2 Free-fall tower tests

An impact test by a free-falling impact projectile with a certain weight is illustrated in Figure 13. The test sample is placed in a enclosed target box to avoid dangers from splinters. The projectile is mounted on the box of weights and elevated to a predetermined height over the test sample. The terminal velocity and kinetic energy of the projectile is controlled by the applied height and weight of the projectile box. Upon release the projectile box falls until hitting the target.

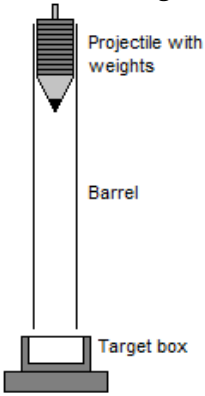

Figure 13: Free-Fall impact test.

This type of impact testing is common and used for a variety of products, for example motorbike helmets as protection against small stones. The calculation for such a facility follows the simply law of kinetic energy E through the mass m and the velocity v of an object:

$$E = \frac{mv^2}{2} \tag{3}$$

The properties of a free fall experiment to simulate a given situation are calculated simply using the basic physical laws of displacement of an accelerated object. Depending on the acceleration *a*, the displacement *s* and the velocity *v* after a time *t* are determined.

$$s(t) = \frac{at^2}{2},\ \dot{s}(t) = v(t) = at,\ \ddot{s}(t) = \dot{v}(t) = a(t) \tag{4}$$

In the case of a free fall tower, the acceleration is equal the gravity *g*. The variables are the drop height and the drop mass. To calculate the kinetic energy of a performed test the drop height is the maximal displacement, s_{max}, and the drop mass is the mass of the projectile box, m_{pbox}. Therefore,

$$E = \frac{m_{pbox}(g\sqrt{\frac{2s_{\max}}{g}})^2}{2} = m_{pbox}s_{\max}g \tag{5}$$

It has to be noted, however, that this calculation allows it to determine the kinetics of a given free-fall tower that operates in a vacuum space. In a normal laboratory environment the projectile box will be obviously object to air resistance, which will reduce the effective acceleration on the projectile box depending on the size of the box as well as the design of the test facility itself.

Moreover, there is a simple possibility to increase the effectiveness of a free-fall tower by accelerating the projectile box mechanically. This can be achieved for example by applying a spring, magnets or an electrical engine.

4.1.3 Highly dynamic impact tests using light-gas guns

As described in the beginning sections, it is important to match an experimental setup as close as possible to the original "real life" situation, provided that it leads to reliable results. In this context, the closest match to a ballistic threat situation is a light-gas gun facility. Light-gas gun facilities utilize pressurized gas to accelerate a projectile equal to that of the ballistic threat in question to exactly simulate the desired case.

Highly dynamic impact tests differ from dynamic impact test by their impact velocity as well as the acceleration applied on the impacting body. Thus, dynamic impact tests normally use a guided projectile, like Charpy's pendulum hammer or the projectile box of a free-fall tower that runs in its tracks. Highly dynamic impact test will commonly accelerate a projectile or impact body to a certain speed and let it hit the target in free flight. The usual equipment to achieve that kind of acceleration is a light-gas gun facility.

An experimental light-gas gun should operate in a similar way to a conventional gun with powder. The main difference is constituted by the means of achieving the necessary pressure to accelerate the projectile. As a conventional gun utilizes the combustion of a propellant charge, a light-gas gun operates with a compressed gas reservoir (Bioletti and Cunningham, 1960; Charters, 1987).

Gas-gun facilities can be applied to simulate a range of different situations, varying with the characteristics of the gun itself. Obviously, since their system was derived from conventional guns, light-gas guns can be used to simulate ballistic impacts of various sizes and energies. Common types of light-gas guns are the one-stage light-gas gun, two-stage light gas gun and the shock tunnel or shock tube. One-stage light-gas guns are rather simple in design, being just one pressure reservoir that accelerates a projectile through a barrel onto the target. The more sophisticated two-stage gun is based on the one-stage gun, but it furthermore has a second stage of compression that increases the pressure in the pressure tank, e.g. by combustion, heating or by free piston compression in an extra tube mounted before the barrel (Doolan and Morgan, 1999; Coolan, 2001). Figure 14 displays schematically the difference between a one-stage light-gas gun and a two-stage light-gas gun with free piston compression. Shock tunnels or shock tubes differ as they do not fire projectiles but only produce a gas blast wave on a target.

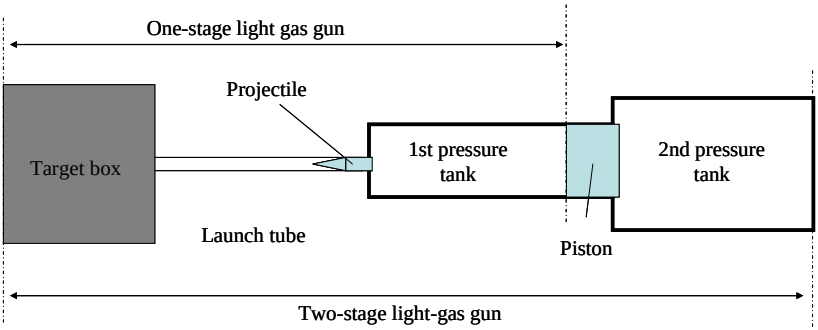

Figure 14: Schematic diagram of a light-gas gun.

Light-gas guns are employed to test materials and composites for their possible application as armors, both for persons and vehicles. On a smaller scale, it is possible to simulate the impact of a stone on a driving vehicle on accelerated velocities, or of ice rocks on a travelling aircraft. Another possible application is to test spacecraft components or materials for their suitability to be used for such a task. There is an ever-growing threat to spacecraft in form of the impact of micrometeoroids and man-made orbital debris. It is estimated that 200 kg of meteoroid mass exist in a distance of 2000 km of the Earth's surface, the majority of it as 0.1-mm micrometeoroids. Additionally, within the same distance around the Earth, there are 300 kg of orbital debris with diameters of less than 1 mm. Those particles are small but they can be found travelling with 10 to 20 km/s relative velocity to an orbiting spacecraft (Kessler et al., 1989). To protect spacecraft and astronauts against the results of an impact at these extremely high velocities these it is necessary to test materials and shielding concepts against these dangers.

Extremely high velocity threats in a laboratory can be simulated using a two-stage light-gas gun system (Grosch and Riegel, 1993). One example for a powerful two-stage gun is displayed in Figure 15. This facility accelerates projectiles with 80 mm diameter to a maximum velocity of 1.2 km/s using an 8 m barrel and a 28.5 dm^3 gas chamber (Georgia Tech). Light-gas guns remain the only equipment able to accelerate projectiles of different shapes and masses to a muzzle velocity of up to 11 km/s (Stilp, 1997).

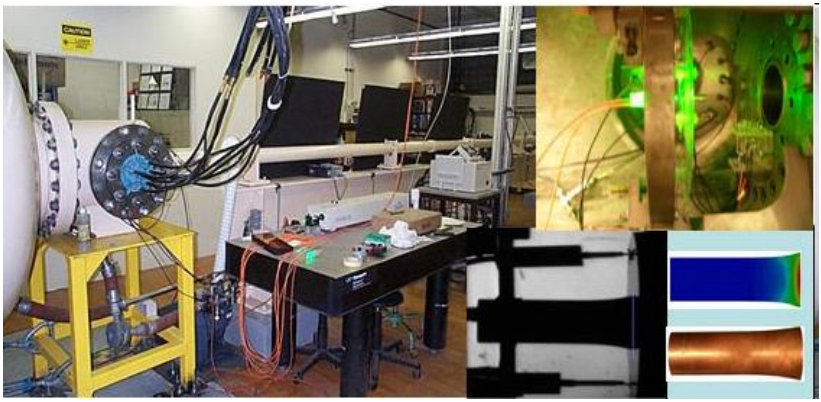

Figure 15: High-strain-rate gas-gun laboratory at Georgia Tech.

It is also possible to conduct tests with light-gas gun equipment to replicate and direct blast waves at test sample or a sensor in a shock tunnel. This allows the simulation of explosions and their effects. It may also be used to examine aerodynamic flow under a wide range of temperatures and pressures, and to study compressible flow phenomena and gas phase combustion reactions. In a more recent approach, biological specimens have been exposed to shock tubes in order to study how they are affected by blast waves (Cernak, 2010; Chavko et al., 2007). One example for a shock tunnel is shown in Figure 16. It is used, for instance, to simulate the reentry of spacecrafts into the atmosphere.

Figure 16: Shock-wind tunnel at Mitsubishi Heavy Industries.

Alternative ways to increase the muzzle velocity are applying a higher pressure in the gas reservoir, increasing the barrel length or heating the driving gas, for example by combustion, arc heating or detonation (Espinosa and Nemat-Nasser, 2000). Still, there remain limitations to the achievable projectile velocities, as the physical properties of the propellant gas, the engineering properties of the facility to withstand the pressure and temperature, and the properties of the projectile itself not to get destroyed by the acceleration force or the base pressure. This is particularly a feature for sabot systems, using a light-mass carrier structure for the projectile in order to increase the diameter without adding too much mass, which can be somewhat problematic. To overcome those problems there are further approaches, e.g., to build multi-staged facilities such as Kondo et al.'s (1999) three-stage light-gas gun.

As shown by various works, different impact velocities will lead to different damage responses even if the kinetic energy of the impacting bodies is equal (Schubel et al., 2005; Zhou and Stronge, 2006). Furthermore, when testing materials for ballistic protection applications, the mechanics to defeat the threat involve destroying partially the projectile (Billon, 1998; Gonçalves et al., 2004; Karandikar et al., 2009).

4.1.4 Theoretical calculation of light-gas gun facilities

The objective of using a light-gas gun facility is to accelerate a projectile to a desired speed, i.e. the muzzle velocity. The acceleration $\dot{v}$ that is subjected on the projectile is determined by its mass *m*, the driving gas pressure *P* and the cross-sectional area as displayed in Equation 6:

$$\dot{v} = \frac{P \cdot A}{m} \tag{6}$$

Seigel (1965) showed that a realistic estimate of the muzzle velocity can be obtained by assuming that the gas reservoir is an infinitely long tube with the same diameter as the barrel thus neglecting reflection and refraction waves in the gas reservoir. In that way the propelling pressure can be related to the projectile velocity *v* by Equation 7:

$$P = P_0[1-(\gamma-1)v/2a_0]^{2\gamma/(\gamma-1)} \tag{7}$$

where P_0 is the initial pressure; γ is the ratio of the specific heat capacities C_P / C_V at constant pressure and constant volume, respectively; and a_0 is the speed of sound in the driving gas.

Reducing the molecular mass of the propelling gas can increase projectile muzzle velocity. The reason for this is that the gas has to be accelerated as well as the projectile. Therefore, a lesser molecular mass means a greater speed of sound and a higher muzzle velocity is achieved. This is because the gas itself has to be accelerated in the same manner as it would be excited by a sound wave. The higher the molecular mass of the gas, the lower the speed of sound and the lower the achievable muzzle velocity. Another factor that has to be taken into account in order to estimate the muzzle velocity is the pressure that is built up in front of the projectile by the atmosphere. This pressure can be described by Equation 8 (Seigel, 1965):

$$\frac{P_t}{P_1} \approx 1+(\frac{v}{a_1})^2 \frac{\gamma_1(\gamma_1+1)}{4} + \frac{\gamma_1 v}{a_1}[1+(\frac{\gamma_1+1}{4})^2(\frac{v}{a_1})^2]^{1/2} \tag{8}$$

where P_t is the pressure that builds up in front of the projectile; P_1 is the initial pressure in front of the projectile, i.e. usually the atmospheric pressure; γ_1 is the ratio of the specific heat capacities of the gas in the barrel and the target chamber, usually air; and a_1 is its speed of sound.

Furthermore, another factor reducing the acceleration of the projectile is the loss of pressure due to the increase of pressured volume, since the projectile travels down the barrel; the driving gas gets distributed over more space. This relation can be expressed by:

$$P = P_0 \frac{V}{V_0}, \tag{9}$$

where V is the volume of the pressurized area at any given moment; and V_0 is the initial volume of the pressure reservoir.

Inserting Equations 7, 8 and 9 in 6 it is possible to calculate the projectile velocity and displacement by iteration in short intervals (Seigel, 1965; Porat and Gvishi, 1980; Brown et al., 1989)

4.1.5 Design of light-gas gun facilities

A simple gas-pressure driven one-stage light-gas gun facility consists basically of a barrel, a gas reservoir as driving force, a chamber to place the projectile, and a mechanism to control the release such as a valve, as shown in Figure 17. Besides the gun itself, it is necessary to set up a suitable target box around the sample, which is constituted by armored walls strong enough to contain the projectile and possible shattered pieces from the impact. The velocity and energy of the projectile depends of the applied pressure as well as the properties of the driving gas, the mass and size of the projectile, the length of the barrel and the size of the reservoir.

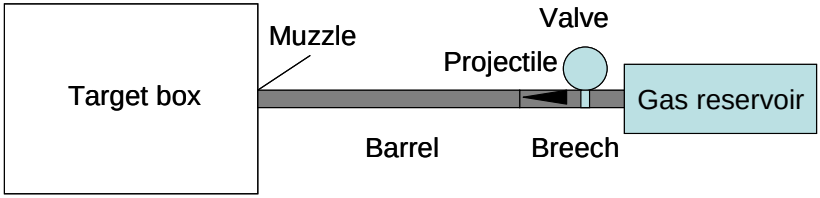

Figure 17: Schematic drawing of a simple one-stage light-gas gun.

Depending on the barrel length, it might be built by joining several segments together. As release mechanisms different systems can be employed. It is possible to use a magnetic valve as well as a diaphragm, e.g., a thin copper foil with a thickness that causes the foil to break as the desired pressure is achieved, see Figure 18 (Hutchins and Winter, 1974).

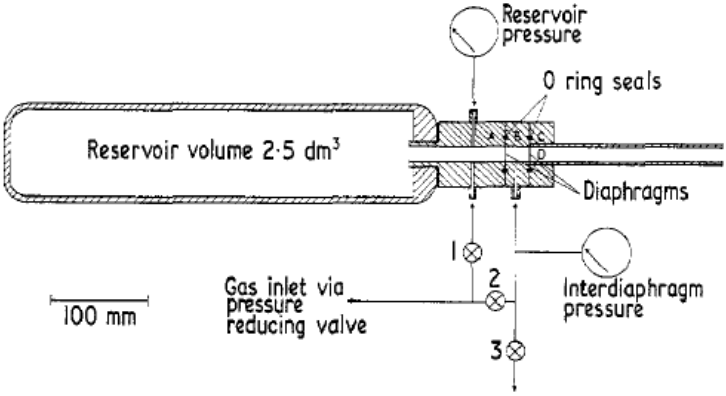

Figure 18: Breech end of a one-stage light-gas gun with diaphragms (Hutchins and Winter, 1974)

The gas reservoir can be either a built pressure tank that is being filled with a gas bottle or by a compressor, or it can be directly the gas bottle itself. Obviously, in latter case the gas bottle should not be bigger than necessary to avoid increased gas usage. Sensors and cameras to record experimental data are to be placed inside the target box as well (Fowles et al., 1970).

One example for a complete design of a one-stage light-gas gun facility as set up by Brown et al. 1989 can be seen in Figure 19. Their design consists of: 1, gas bottle; 2, gas regulator; 3, control box; 4, three-way valve; 5, gas line (two barrel connections); 6, gas vent line; 7, solenoid activation cable; 8, pressure gauge; 9, pressure vessel; 10, leak valve; 11, solenoid valve; 12, ball joint; 13, breech; 14, barrel; 15, hardened wall: 16, blast screen; 17, incident velocity device; 18, target support stand: 19, exit velocity device; and 20, catcher box (Brown et al., 1989).

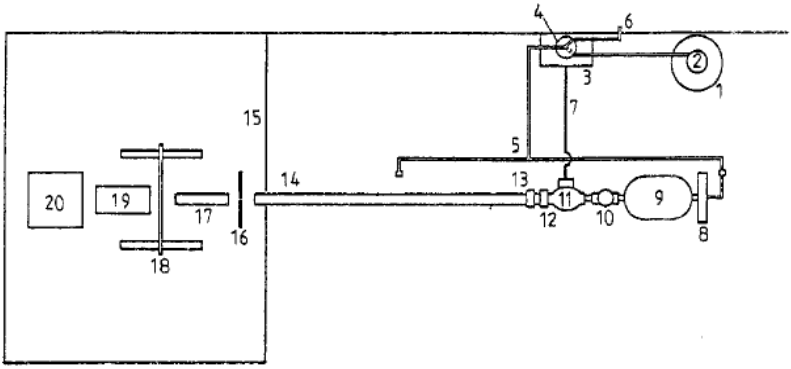

Figure 19: Schematic diagram of a gas-gun facility (Brown et al., 1989).

5 RESULTS

In the following sections the obtained numerical results for dynamic and highly dynamic impact tests will be displayed and analyzed.

5.1 DYNAMIC IMPACT TEST

Impact tests such as the Charpy or Izod Impact tests are designed to test small samples with a predetermined geometry. In order to test complete structures or composite materials it might be necessary to employ other means of impact testing, one of the most common ones being the free-fall tower equipment. The numerical calculation of the required drop mass and drop height to achieve an equal kinetic energy on impact as desired is shown in Section 4.1.2.2. The necessary drop masses for different heights are displayed in

Table 5 to achieve the same impact energy as the ballistic threats according to NIJ categorization. The first three tables consider a "pure" free-fall tower apparatus, while the last table is calculated with a higher artificial additional acceleration to increase the kinetic energy. The first part of the table shows the necessary drop mass to the reach kinetic energy for every threat level for a drop height of 1.5 m. To successfully reach the characteristics of a level III threat already 234.26 kg are required; as noted before this applies to a perfect system without losses due air resistance and friction. At a drop height of 2.0 m and 2.5 m the drop masses are reduced to 175.69 kg and 140.55 kg, respectively. The usage of an artificial additional acceleration allows the reduction of the applied drop mass further to 91.81 kg.

Table 5: Free-fall tower calculation examples

CALCULATION WITH 1.5m DROP HEIGHT									
Simulated Test Properties					Free Fall Tower Properties				
Type	Caliber	Mass [g]	Speed [m/s]	Energy [J]	Drop Height [m]	Acceleration [m/s²]	Time until impact [s]	Final speed [m/s]	Drop mass [kg]
Type IIA	9 mm FMJ RN	8.00	373.00	556.52	1.50	9.80	0.55	5.42	37.86
	.40 S&W FMJ	11.70	352.00	724.84	1.50	9.80	0.55	5.42	49.31
Type II	9 mm FMJ RN	8.00	398.00	633.62	1.50	9.80	0.55	5.42	43.10
	.357 Magnum JSP	10.20	436.00	969.49	1.50	9.80	0.55	5.42	65.95
Type IIIA	.357 SIG FMJ FN	8.10	448.00	812.85	1.50	9.80	0.55	5.42	55.30
	.44 Magnum SJHP	15.60	436.00	1482.75	1.50	9.80	0.55	5.42	100.87
Type III	7.62 mm FMJ (M80)	9.60	847.00	3443.56	1.50	9.80	0.55	5.42	234.26
Type IV	.30 AP (M2 AP)	10.80	878.00	4162.77	1.50	9.80	0.55	5.42	283.18
CALCULATION WITH 2.0m DROP HEIGHT									
Simulated Test Properties					Free Fall Tower Properties				
Type	Caliber	Mass [g]	Speed [m/s]	Energy [J]	Drop Height [m]	Acceleration [m/s²]	Time until impact [s]	Final speed [m/s]	Drop mass [kg]
Type IIA	9 mm FMJ RN	8.00	373.00	556.52	2.00	9.80	0.64	6.26	28.39
	.40 S&W FMJ	11.70	352.00	724.84	2.00	9.80	0.64	6.26	36.98
Type II	9 mm FMJ RN	8.00	398.00	633.62	2.00	9.80	0.64	6.26	32.33
	.357 Magnum JSP	10.20	436.00	969.49	2.00	9.80	0.64	6.26	49.46
Type IIIA	.357 SIG FMJ FN	8.10	448.00	812.85	2.00	9.80	0.64	6.26	41.47
	.44 Magnum SJHP	15.60	436.00	1482.75	2.00	9.80	0.64	6.26	75.65
Type III	7.62 mm FMJ (M80)	9.60	847.00	3443.56	2.00	9.80	0.64	6.26	175.69
Type IV	.30 AP (M2 AP)	10.80	878.00	4162.77	2.00	9.80	0.64	6.26	212.39
CALCULATION WITH 2.5m DROP HEIGHT									
Simulated Test Properties					Free Fall Tower Properties				
Type	Caliber	Mass [g]	Speed [m/s]	Energy [J]	Drop Height [m]	Acceleration [m/s²]	Time until impact [s]	Final speed [m/s]	Drop mass [kg]
Type IIA	9 mm FMJ RN	8.00	373.00	556.52	2.50	9.80	0.71	7.00	22.71
	.40 S&W FMJ	11.70	352.00	724.84	2.50	9.80	0.71	7.00	29.59
Type II	9 mm FMJ RN	8.00	398.00	633.62	2.50	9.80	0.71	7.00	25.86
	.357 Magnum JSP	10.20	436.00	969.49	2.50	9.80	0.71	7.00	39.57
Type IIIA	.357 SIG FMJ FN	8.10	448.00	812.85	2.50	9.80	0.71	7.00	33.18
	.44 Magnum SJHP	15.60	436.00	1482.75	2.50	9.80	0.71	7.00	60.52
Type III	7.62 mm FMJ (M80)	9.60	847.00	3443.56	2.50	9.80	0.71	7.00	140.55
Type IV	.30 AP (M2 AP)	10.80	878.00	4162.77	2.50	9.80	0.71	7.00	169.91
CALCULATION WITH 2.5m DROP HEIGHT AND ARTIFICIAL ACCELERATION									
Simulated Test Properties					Free Fall Tower Properties				
Type	Caliber	Mass [g]	Speed [m/s]	Energy [J]	Drop Height [m]	Acceleration [m/s²]	Time until impact [s]	Final speed [m/s]	Drop mass [kg]
Type IIA	9 mm FMJ RN	8.00	373.00	556.52	2.50	15.00	0.58	8.66	14.84
	.40 S&W FMJ	11.70	352.00	724.84	2.50	15.00	0.58	8.66	19.33
Type II	9 mm FMJ RN	8.00	398.00	633.62	2.50	15.00	0.58	8.66	16.90
	.357 Magnum JSP	10.20	436.00	969.49	2.50	15.00	0.58	8.66	25.85
Type IIIA	.357 SIG FMJ FN	8.10	448.00	812.85	2.50	15.00	0.58	8.66	21.68
	.44 Magnum SJHP	15.60	436.00	1482.75	2.50	15.00	0.58	8.66	39.54
Type III	7.62 mm FMJ (M80)	9.60	847.00	3443.56	2.50	15.00	0.58	8.66	91.83
Type IV	.30 AP (M2 AP)	10.80	878.00	4162.77	2.50	15.00	0.58	8.66	111.01

5.2 HIGHLY DYNAMIC IMPACT TESTING

Using equations 6 through 9, the possible accelerations and muzzle velocities have been calculated for a one-stage light-gas gun facility considering the specifications on projectiles for Level III threats (i.e. a FMJ projectile with 9.6 g mass and 7.62 mm diameter). Besides that, the maximum available pressure for the gas reservoir has been fixed as 20 N/mm², which is the pressure of standard industrial gas bottles. The obtained results are presented and discussed below.

Table 6: Achievable muzzle velocities (I)

Projectile according to Level III threat (7.62 mm diameter; 9.6 g weight)						
Gas	V_{max} (m/s)	Barrel length [m]	V_{3m} [m/s]	V_{6m} [m/s]	Pressure [N/mm²]	Reservoir [cm³]
Nitrogen	527.99	29.88	378.51	442.19	20.00	1000.00
Helium	849.71	40.52	511.96	631.83	20.00	1000.00
Hydrogen	1054.78	46.74	571.28	725.14	20.00	1000.00

Table 6 shows different possible set-ups with different barrel lengths, diameters and driving gases. The reservoir size was set as 1 liter. It is easy to see that hydrogen-driven projectiles achieve higher velocities than nitrogen or helium-driven ones. The reason for this lies in the different speeds of sound of the gases, as explained before. V_{max} is the maximum velocity achievable for the respective set-up, which is reached at the given barrel length. If a longer barrel would be applied, then the counter pressure in front of the projectile would result in a higher deceleration than the remaining pressure in the reservoir and the barrel, so that the muzzle velocity would actually be lower for even longer barrels.

The maximal achievable velocities using helium and hydrogen would be sufficient for Level III and, in the case of hydrogen, even for Level IV tests. However, barrel lengths of over 40 m are far from being reasonable. Apart from the space, such facility would require constructing a barrel without leakage, completely plane and leveled, what would render such a design unfit to serve the desired motivation of constructing a simple assembly. The muzzle velocities for reasonable barrel lengths as 3 m and 6 m are shown in Table 6, as V_{3m} and V_{6m} values. Therefore, even using hydrogen as propellant gas and a 6 m long barrel it is not possible to achieve the desired muzzle velocity of 847 m/s for level III testing.

Table 7: Achievable muzzle velocities (II)

Projectile according to Level III threat (7.62 mm diameter; 9.6 g weight)						
Gas	V_{max} (m/s)	Barrel length [m]	V_{3m} [m/s]	V_{6m} [m/s]	Pressure [N/mm²]	Reservoir [cm³]
Nitrogen	564.22	39.22	382.31	450.60	20.00	2500.00
Helium	934.14	52.79	517.89	646.69	20.00	2500.00
Hydrogen	1187.90	61.34	578.38	744.20	20.00	2500.00
Nitrogen	584.19	47.72	384.07	453.41	20.00	5000.00
Helium	982.84	64.08	521.02	653.54	20.00	5000.00
Hydrogen	1268.56	74.78	582.33	750.10	20.00	5000.00

Table 7 shows the results for larger gas reservoirs. Although the maximal speeds are increased, they come with even longer barrels. The achievable muzzle velocities with 3 m and 6 m barrels do not differ

highly from those with big reservoirs. The larger reservoir results in a slower decrease in acceleration pressure and therefore acceleration force is higher than the counter pressure for a longer time. In this way, the muzzle velocity increases with a 3 m barrel and nitrogen from 378.51 m/s (100% at 1000 cm³) to 382.31 m/s (101% at 2500 cm³) to 384.07 m/s (101.5% at 5000 cm³). The increase is slightly higher with a 6 m long barrel, 102% with 2500 cm³ and 102.5% with 5000 cm³.

Based on these calculations, there are three options to achieve the desired muzzle velocities. The first option is to change the design to a two-stage light-gas gun facility. A second stage would increase the pressure in the gas reservoir further and therefore allow higher muzzle velocities. Another way would be to directly use higher pressures. In that case a compressor would have to be employed as a part of the facility since standard industry gas cylinders do not supply higher pressures. The third option would be to employ a sabot as a carrier of the projectile, thus increasing the diameter of the accelerated object without adding significantly mass, as Grosch (1993) and Borvik (1999) did. In that case, assuming a sabot mass of 5 g and 10 g to increase the bore diameter of the facility to 40 mm, the calculations are shown in Table 8. In this case, the performance will depend majorly on the sabot mass. The upper part of Table 8 shows the results with a sabot that would add a mass of 5 g to the projectile, while the lower part was calculated for a sabot of 10 g. In both cases only with hydrogen as driving gas it is possible to achieve speeds for Level III tests.

Table 8: Achievable muzzle velocities (III)

Projectile according to Level III threat with 5 g Sabot (40mm diameter; 14.6 g weight)						
Gas	Vmax (m/s)	Barrel length [m]	V3m [m/s]	V6m [m/s]	Pressure [N/mm²]	Reservoir [cm³]
Nitrogen	510.61	1.40	-	-	20.00	1000.00
Helium	807.61	2.00	-	-	20.00	1000.00
Hydrogen	988.71	2.31	-	-	20.00	1000.00
Projectile according to Level III threat with 5 g sabot (40 mm diameter; 14.6 g weight)						
Gas	Vmax (m/s)	Barrel length [m]	V3m [m/s]	V6m [m/s]	Pressure [N/mm²]	Reservoir [cm³]
Nitrogen	551.01	1.85	-	-	20.00	2500.00
Helium	901.18	2.61	-	-	20.00	2500.00
Hydrogen	1133.42	3.00	1133.42	-	20.00	2500.00
Projectile according to Level III threat with 10 g sabot (40mm diameter; 19.6 g weight)						
Gas	Vmax (m/s)	Barrel length [m]	V3m [m/s]	V6m [m/s]	Pressure [N/mm²]	Reservoir [cm³]
Nitrogen	493.94	1.73	-	-	20.00	1000.00
Helium	771.79	2.42	-	-	20.00	1000.00
Hydrogen	936.31	2.79	-	-	20.00	1000.00
Projectile according to Level III threat with 10 g sabot (40 mm diameter; 19.6 g weight)						
Gas	Vmax (m/s)	Barrel length [m]	V3m [m/s]	V6m [m/s]	Pressure [N/mm²]	Reservoir [cm³]
Nitrogen	538.41	2.32	-	-	20.00	2500.00
Helium	872.19	3.15	871.79	-	20.00	2500.00
Hydrogen	1088.17	3.65	1082.25	-	20.00	2500.00

Due to the increase of the bore diameter, the reservoir of 1000 cm³ is rather small, since the absolute volume of the area under pressure increases much faster with every travelled distance unit. Table 8 shows an increase to 108%, 112% and 115% for nitrogen, helium and hydrogen, respectively, considering a 5 g sabot, and 109%, 113% and 116% with a 10 g sabot and a reservoir of 2500 cm³. Furthermore, the optimal barrel length to achieve the maximal muzzle velocity has increased. With such a configuration it is possible to achieve the velocity for level III tests of 847 m/s using helium or hydrogen and a sabot of either 5 or 10 g.

Still, it is not possible to determine if the chosen value of 40 mm for the sabot diameter is optimal. Figure 20 and Table 9 show the development of the velocities with different sabot diameters, the sabot mass being fixed at 10 g in addition to the 9.6 g of the projectile. As can be seen, the sabots of 35 mm and 30 mm diameter seem to perform better when considering nitrogen as propellant gas (Figure 20 (a)). However, with the other two driving gases the 40 mm sabot still achieve higher muzzle velocities with a 3 m or less barrel length (Figure 20 (b) and (c)).

Table 9: Achievable muzzle velocities (IV)

Projectile according to Level III threat with different diameter sabot (10 g each, 19.6 g total weight)						
Gas	V_{max} (m/s)	Barrel length [m]	V_{3m} [m/s]	Sabot diamter [mm]	Pressure [N/mm²]	Reservoir [cm³]
Nitrogen	538.41	2.32	-	40.00	20.00	2500.00
Nitrogen	550.37	2.47	-	35.00	20.00	2500.00
Nitrogen	549.90	3.36	549.37	30.00	20.00	2500.00
Nitrogen	549.56	4.92	539.48	25.00	20.00	2500.00
Nitrogen	549.33	7.64	514.70	20.00	20.00	2500.00
Nitrogen	549.18	13.62	469.95	15.00	20.00	2500.00
Nitrogen	549.08	30.63	392.62	10.00	20.00	2500.00
Projectile according to Level III threat with different diameter sabot (10 g each, 19.6 g total weight)						
Gas	V_{max} (m/s)	Barrel length [m]	V_{3m} [m/s]	Sabot diamter [mm]	Pressure [N/mm²]	Reservoir [cm³]
Helium	872.19	3.15	871.79	40.00	20.00	2500.00
Helium	871.52	4.16	862.35	35.00	20.00	2500.00
Helium	871.04	5.65	836.01	30.00	20.00	2500.00
Helium	870.71	8.14	794.33	25.00	20.00	2500.00
Helium	870.49	12.77	725.36	20.00	20.00	2500.00
Helium	870.34	22.66	625.66	15.00	20.00	2500.00
Helium	870.26	50.98	485.79	10.00	20.00	2500.00
Projectile according to Level III threat with different diameter sabot (10 g each, 19.6 g total weight)						
Gas	V_{max} (m/s)	Barrel length [m]	V_{3m} [m/s]	Sabot diamter [mm]	Pressure [N/mm²]	Reservoir [cm³]
Hyrdogen	1088.17	3.65	1082.25	40.00	20.00	2500.00
Hyrdogen	1087.50	4.88	1060.50	35.00	20.00	2500.00
Hyrdogen	1087.06	6.61	1013.91	30.00	20.00	2500.00
Hyrdogen	1086.79	9.46	949.99	25.00	20.00	2500.00
Hyrdogen	1086.62	14.73	850.53	20.00	20.00	2500.00
Hyrdogen	1086.54	26.24	715.97	15.00	20.00	2500.00
Hyrdogen	1086.50	58.92	535.31	10.00	20.00	2500.00

(a)

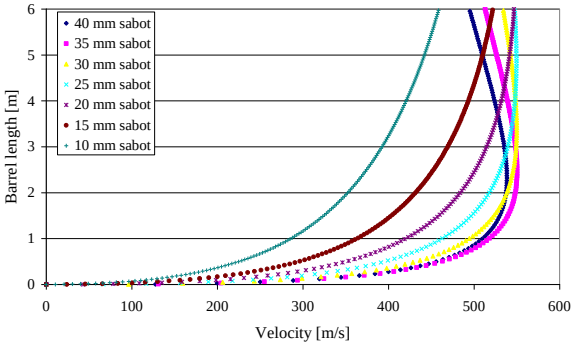

(b)

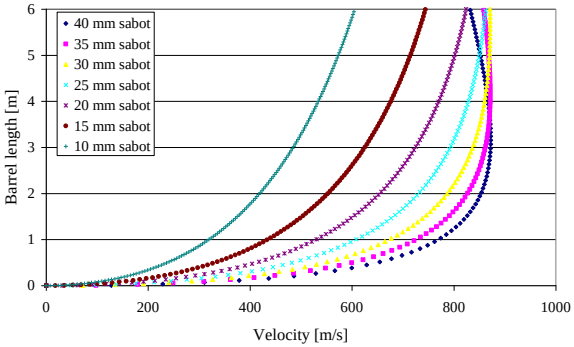

(c)

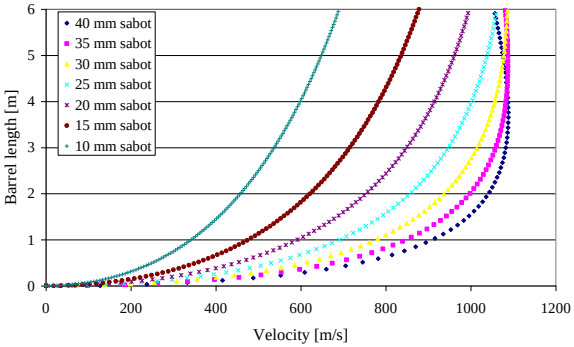

Figure 20: Sabot performance: Sabot/projectile velocity against displacement with driving gas a) nitrogen, b) helium and c) hydrogen

6 DISCUSSION

The obtained results and conclusions from the studied literature and the conducted calculations show two answers about the material testing for impact properties.

6.1 INFLUENCE OF THE RATIO BETWEEN IMPACT MASS AND VELOCITY

The first question is whether it is of advantage or even necessary to apply a test which uses not only an equal kinetic energy but also an equal impact velocity to positively simulate a given impact scenario. As shown by Zhou and Stronge (2006) the impact velocity has an influence on the impact force of the projectile even if the kinetic energy is considered constant. Evci and Güglec (2012) found that the material strength of composites is significantly higher for higher loading rates.

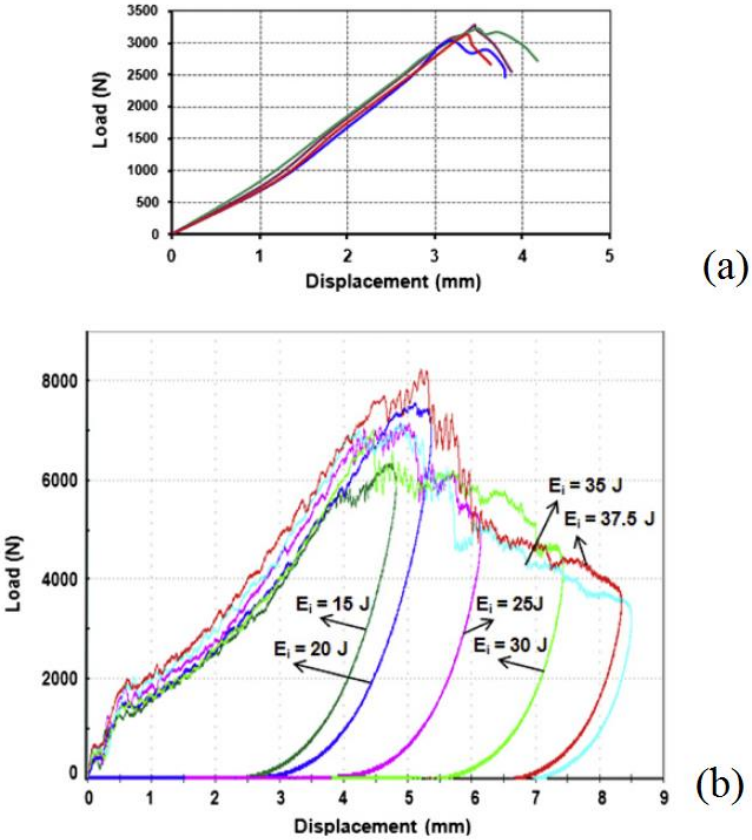

Figure 21: Load-displacement curves of composite test specimens subjected to (a) quasi-static (bending tests), (b) dynamic (low velocity impact) loading (Evici and Güglec, 2012).

Figure 21 shows the load-displacement curves of composite specimens in quasi-static three-point bending tests as a) while b) displays the load-displacement curves in dynamic drop-weight tests with kinetic energies up to 37.5 J. The slopes of the ascending curves of dynamic loading are twice as high as the slopes of the curves of the static loading case. Also, load bearing capacity in dynamic loading increases up to 2.5 times. The tested specimens were woven E-Glass composite specimens; with other materials Evci and Güglec (2012) were even able to obtain higher differences.

In the area of high impact test it is also important to consider the influence of the projectile mass; since the defeat mechanism of a given armor system against a projectile threat involves the at least partial destruction of the projectile body. Thus the projectile mass is reduced, and, together with it, the kinetic energy. As shown by Gonçalves (2004) and Neckel (2010) a high part of the kinetic energy is defeated that way. Since a free-fall tower utilizes projectile boxes of a far higher mass and a lower velocity, this mass reduction of the projectile would have a much lower influence on the damage behavior.

Therefore it is necessary to use the most appropriate test facility to obtain results that match the corresponding real scenario most fittingly. For the presented question of a ballistic protection system, the logical device is a light-gas gun.

6.2 LIGHT-GAS GUN FACILITY TO SIMULATE LEVEL III / IV BALLISTIC THREATS

As described before there are different types of light-gas guns that differ in size and complexity. The aim of this work is to evaluate the possibility to use the simplest setup for the task to simulate level III / IV ballistic threats. The one-stage light-gas gun is definitely the least complex version, but also the least powerful as compared to two- or even three-stage light-gas guns. When respecting limiting factors like reasonable barrel lengths, not more than 6 meters, and standard industrial pressure bottles as pressure reservoir, maximum pressure of 20 N/mm², showed a severe lack of power to accelerate a 9.6 g projectile to the requested 847 m/s. None of the three gases investigated as driving gas, nitrogen, helium and hydrogen, are able to provide the desired acceleration force. The maximum achievable velocities are for Nitrogen with 442.19 m/s at 52.2% of the desired velocity, for helium with 631.83 m/s at 74.6% and for hydrogen with 725.14 m/s at 85.6 m/s.

On the other hand, using light-mass carriers to increase the diameter of the barrel without adding much to the mass it is possible to achieve the desired velocities, at least with helium or hydrogen as driving gas. With helium it is possible to achieve a muzzle velocity of 871.19 m/s while hydrogen permits to accelerate the projectile to up to 1088.17 m/s. Besides easily reaching the desired the velocities the usage of sabots opens further promising possibilities. To change the shape of a sabot to adjust it to other projectiles with different shapes and masses is much easier than to build a new barrel to connect to the facility. By reducing the driving pressure it is possible to adjust the system also to

projectile of less mass or for lower velocities. DeRose and Intriere (1970) present a huge variety of different sabots from NASA laboratories, used to accelerate projectiles, miniature planes or shuttles, particles and more.

Interesting to see is the comparison of the achievable maximum velocities: For either gas the maximum velocity is nearly independent of the sabot diameter – as long as the barrel can be any given length and the weight is constant. Of course, it has to be noticed that in this calculation the mass of the sabot has been taken as fixed; a sabot of a higher diameter will also put up a higher additional mass to the projectile.

7 CONCLUSION AND SUGGESTIONS FOR FUTURE WORKS

It has been shown that the impact velocity may have a high influence on the damage outcome of an impact. Even if an equal kinetic energy is applied, a higher velocity leads to a higher impact force than a lower one. Furthermore the defeat mechanisms are different for threats with high velocity and low weight in comparison to low velocity and high weight.

Different set ups for a one-stage light-gas gun facility have been numerically analyzed in order to evaluate their suitability for usage to test materials and composites for NIJ Level III and IV armor protection. A maximal barrel length of 6 m and a maximal reservoir pressure of a standard industrial gas bottle (20 N/mm^2) have been chosen as limitations. The numerical predictions show, that it is not possible to accelerate the projectile directly to the desired velocity with nitrogen, helium or hydrogen as propellant gas without greatly surpassing the pressure limitations.

The calculations have shown that it is possible to build a simple one-stage light-gas gun to achieve an exact replication of level III or level IV ballistic threats and therefore carry through precise testing, if using a light-weight carrier as sabot. A sabot also provides an increased flexibility to the facility to test different bodies as impacting force on sample material.

Future works should include an investigation of different designs for sabot to achieve a high resistance while maintaining a low weight. A fragile sabot assembly will not even survive the travel down the barrel, but rather break before. Thus, the possibility of reclaiming the sabot without damage and reusing it is advisable for sabot design.

Another topic would be to examine the different damage results of a free-fall tower and a light-gas gun facility to see if a correlation can be obtained. As shown in this work, the outcomes will be different for equal kinetic energy impacts. Nevertheless, if a correlation can be found to calculate a transition between the results of the two alternative systems, it could be possible to successfully apply also dynamic impact tests to obtain results for high velocity impact situations.

REFERENCES

BILLON, H.: A Model for Ballistic Impact on Soft Armour, DSTO Aeronautical and Maritime Research Laboratory, DSTO-TR-0730, 1998

BIOLETTI, C.; Cunningham, B.E.: A high velocity gun employing a shock compressed light gas, NASA Technical Note D-307, 1960

BODYARMORNEWS.COM: Bulletproof Vests - How Are Bulletproof Vests Made?, http://www.bodyarmornews.com/bulletproof-vests.htm, accessed at 05th December, 2012

BORVIK, T.; Langseth, M.; Hopperstad, O. S.; Malo, K. A.: Ballistic penetration of steel plates, International Journal of Impact Engineering Vol. 22, 1999, pp. 855-886

BROWN, J.R.; Chappell, P.J.C; Egglestone, G.T.; Gellert, E.P.: A gas-gun facility for material impact studies using low-velocity, low-mass projectiles, Journal for Physics E: Scientific Instruments Vol. 22, 1989, pp. 771-774

BUNDESARCHIV Bild 102-12610, Kugelsichere Weste, 1931 http://upload.wikimedia.org/wikipedia/commons/5/5d/Bundesarchiv_Bild_102-12610%2C_Kugelsichere_Weste.jpg, accessed at 29th November 2012

BURGOS-MONTES, O.; Moreno, R.; Baudín, C.: Effect of mullite additions on the fracture mode of alumina, Journal of the European Ceramic Society Vol. 30, 2010, pp. 857–863

CALLISTER JR., W.D.: Materials Science and Engineering: An Introduction, 7th Edition, John Wiley & Sons, Inc., 2007

CERNAK, I.: The importance of systemic response in the pathobiology of blast-induced neurotrauma, Frontiers in Neurology Vol. 1, 2010, pp. 1-9

CHARTERS, A.C.: Development of the high-velocity gas-dynamics gun, International Journal of Impact Engineering Vol. 5, 1987, pp. 181-203

CHAVKO, M.; Koller, W.A.; Prusaczyk, W.K.; McCarron, R.M.: Measurement of blast wave by a miniature fiber optic pressure transducer in the rat brain, Journal of Neuroscience Methods Vol. 159, 2007, pp. 277-281

CONCEPT BLINDAGENS: Proteção a prestação: blindados mais perto da classe média, http://www.conceptblindagens.com.br/artigos/protecao-a-prestacao-blindados-mais-perto-da-classe-media, accessed at 29th November 2012
and: Direção de veículo blindado exige cuidados especiais,

http://www.conceptblindagens.com.br/artigos/direcao-de-veiculo-blindado-exige-cuidados-especiais, accessed at 29th November 2012
CONNOR, P.: Ballistic Protection Industry; Are Today's Niche Players Tomorrow's Market Leaders? ,Frost & Sullivan Market Insights, 2006., http://www.frost.com/sublib/display-market-insight-top.do?id=88515799, accessed at 29th November 2012
COOLAN, C.: A Two-Stage Light Gas Gun for the Study of High Speed Impact in Propellants, DSTO Aeronautical and Maritime Research Laboratory, DSTO-TR-1092, 2001
DEROSE, C.E.; Intrieri, P.F.: Model and sabot design and launching techniques; AGARD Ballistic Range Technology, Aug. 1970, P 97-154
DOOLAN, C.J.; Morgan, R.G.: A two-stage free-piston driver, Shock Waves Vol. 9, 1999, pp. 239-248
ENGINEERED MATERIALS HANDBOOK VOL. 4: Ceramics and Glasses, Vol. Chairman Schneider Jr., S.J.; ASM Intgernational, 1991
ESPINOSA, H.D.; Nemat-Nasser, S.: Low-Velocity Impact Testing, ASM-Handbook Vol. 8, 2000, pp. 539-559
EVCI, C.; Güglec, M.: An experimental investigation on the impact response of composite materials, International Journal of Impact Engineering, Vol. 43, 2012, pp. 40-51
FAWAZ, Z.; Zheng, W.; Bedinan, K.: Numerical simulation of normal and oblique ballistic impact on ceramic composite armours, Composite Structures, Vol. 63, 2004, pp. 387–395
FOWLES, G.R.; Duvall, G.E:; Asay, J.; Bellamy, P.; Feistmann, F.; Grady, D.; Michaels, T.; Mitchell, R.: Gas Gun for Impact Studies, The Review of Scientific Instruments Vol. 41, 1970, pp. 984-996
GEORGIA TECH COLLEGE OF ENGINEERING, High strain-rate gas laboratory, http://www.mse.gatech.edu/research/equipment-facilities/high-strain-rate-gas-gun-laboratory, accessed at 05.11.2012
GONÇALVES, D.P.; Melo, F.C.L.; Klein, A.N.; Al-Qureshi, H.A.: Analysis and investigation of ballistic impact on ceramic/metal composite armour, International Journal of Machine Tools & Manufacture Vol. 44, 2004, pp. 307-316
GROSCH, J.D.; Riegel, J.P.: Development and Optimization of a Micro Two-Stage Light-Gas Gun, International Journal of Impact Engineering Vol. 14, 1993, pp.315-324

HUTCHINGS, I.M.; Winter, R.E.: A simple small-bore laboratory, Journal for Physics E: Scientific Instruments Vol. 8, 1974, pp 84-85

KARANDIKAR, P.G.; Evans, G.; Wong, S.; Aghajanian, M.K.: A Review of ceramics for armor applications, Advances in Ceramic Armor IV: Ceramic Engineering and Science Proceedings, Volume 29, Issue 6, 2009, pp. 163-175

KESSLER, D. J.; Reynolds, R. C.; Anz-Meader, P. D.: Orbital Debris Environment for Spacecraft Designed to Operate in Low Earth Orbit. NASA Technical Memorandum 100471, 1989

KONDO, K.; Fat'yanov, O.V.; Hironaka, Y.; Moritoh, T.; Ozaki, S.: Performance of the three-stage light-gas gun with a preheating stage, CP505, Shock Compression of Condensed Matter, 1999, pp. 1167-1170

KURISHITA H.; Kayano H.; Narui M.; Yamazaki M.; Kano Y.; Shibahara I.: (1993). Effects of V-notch dimensions on Charpy impact test results for differently sized miniature specimens of ferritic steel, Materials Transactions - Japan Institute of Metals, Vol. 34, 1993, pp. 1042–52

LUBLINER, J.: Plasticity Theory, Macmillan Publishing Company, New York, 1990

LUNDBERG, P.; Renström, R.; Lundberg, B.: Impact of metallic projectiles on ceramic targets: Transition between interface defeat and penetration, International Journal of Impact Engineering, Vol. 24, 2000, pp. 259-275

MAENSIRI, S.; Roberts S.G.: Thermal shock of ground and polished alumina and Al2O3/SiC nanocomposites, Journal of the European Ceramic Society, Vol. 22, 2002, pp. 2945–2956

MATHURT K.K.; Needleman A.; Tvergaard V.: Analysis of failure modes in the Charpy impact test, Modeling and Simulation in Materials Science Engineering Vol. 2, 1994, pp. 617-635

MEYERS, M.A.; Chawla, K.K.: Mechanical Behaviors of Materials. Prentice Hall, 1998

MILLS, N.J.: The mechanism of brittle fracture in notched impact tests on polycarbonate, Journal of Materials Science Vol. 11, 1976, pp. 363–375

MITSUBISHI HEAVY INDUSTRY LTD., Shock Tunnel Test Facility, http://www.mhi.co.jp/en/products/detail/shock_wind_tunnel.html , accessed at 05.11.2012

MOTORTREND: Mercedes Benz Museum Tour 1935 Mercedes Benz 770 Pullman Limo Emperor Hirohito, 2006,

http://m.motortrend.com/features/112_0607_mercedes_benz_museum_tour/photo_16.html, accessed at 20th October 2011
NADLER, C.W.: Mid-15th Brigandine remodeled armor, 2006, http://nadler.us/brig_craig1.html accessed at 05th December 2012
NATIONAL INSITUTE OF JUSTICE (NIJ), United States Department of Justice: Ballistic Resistance of Body Armor, National Institute of Justice Standard-0101.06, 2006
NATIONAL MUSEUM OF AFRICAN ART (NMAFA): Hausa armed horsemen in quilted armor at Independence Day celebration, http://africa.si.edu/exhibits/styles/identity2.html, accessed at 05th December 2012
NECKEL, L.: Modelamento e simulação de impacto balístico em sistema cerâmica-metal, Florianópolis: Universidade Federal de Santa Catarina, Biblioteca Universitária, 2012.
ONG, C.W.; Boey, C.W.; Hixson, R.S.; Sinnibaldi, J.O.: Advanced layered personnel armor, International Journal of Impact Engineering, Vol. 38, 2011, pp. 369-383
PORAT, Y ; Gvishi, M: The performance of a short-barrelled gas gun, Journal for Physics E: Scientific Instruments Vol. 13, 1980, pp 504-505
SCHUBEL, P.M.; Luo, J.-J.; Daniel, I.M.: Low velocity impact behavior of composite sandwich panels, Composites Part A: Applied Science and Manufacturing, Volume 36, 2005, pp. 1389-1396
SEIGEL, A.E., The theory of high speed guns, NATO AGARdograph 91, 1965
SNILES, A.: History of Ceramics, http://ceramics.org/learn-about-ceramics/history-of-ceramics, The American Ceramics Society May 20th, 2009
STILP, A.J.: Hyper Velocity Impact Research, Proceeding of the Second European Conference on Space Debris, ESA SP-393, 1997
SUBSTANCES & TECHNOLOGIES (SubsTech), Flexural strength tests of ceramics, http://www.substech.com/dokuwiki/doku.php?id=flexural_strength_tests_of_ceramics, accessed at 04th December 2012
TASDEMIRCI, A.; Tunusoglu, G.; Güden, M.: The effect of the interlayer on the ballistic performance of ceramic/composite armors: Experimental and numerical study, International Journal of Impact Engineering, Vol. 44, 2012, pp. 1-9

VISWANATHAN, R.: Damage Mechanisms and Life Assessment of High-Temperature Components, ASM Internetional, 1995

ZHOU, D.W.; Stronge, W.J.: Ballistic limit for oblique impact of thin sandwich panels and spaced plates, International Journal of Impact Engineering Vol. 35, 2008, pp. 1339-1354

ZHOU, D.W.; Stronge, W.J.: Low velocity impact denting of HSSA lightweight sandwich panel, International Journal of Mechanical Sciences Vol. 48, 2006, pp. 1031-1045

APPENDIX A

PROJECT: CONSTRUCTION OF A SIMPLE LIGHT-GAS GUN FOR NIS LEVEL III AND IV TESTS OF MATERIALS AND COMPOSITES FOR ARMOR APPLICATIONS.

The following pages aim to describe possible solutions for the requirements to build a one-stage light-gas gun according to the descriptions and specifications that have been presented in the dissertation.

Necessary parts for a light-gas gun are the following:

- Pressure reservoir
- Gas source
- Trigger mechanism
- Projectile housing
- Barrel
- Target box
- Target inlet

Additionally equipment should be installed for safety, evaluation and performance purposes:

- Optical sensors to measure velocity
- High speed camera
- For sabot-operation: catching mechanism to separate sabot and projectile (only for some sabot designs)
- Sabots

This suggested design's main components are assembled in Figure 1. Figure 2 gives a more detailed view on the projectile housing.

Figure 1: One-stage light-gas gun design

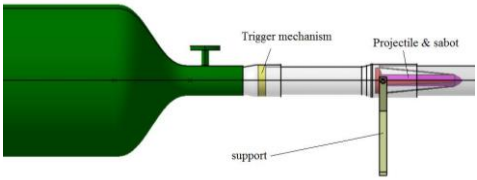

Figure 2: One-stage light-gas gun: Projectile housing

The necessary conditions for those parts to achieve the desired ballistic properties are presented in Table 1.

Table 1: Achieveable muzzle velocities with sabot and 2.5 l gas reservoir

Projectile according to Level III threat with different diameter sabot (10 g each, 19.6 g total weight)						
Gas	V_{max} (m/s)	Barrel length [m]	V_{3m} [m/s]	Sabot diamter [mm]	Pressure [N/mm²]	Reservoir [cm³]
Nitrogen	538.41	2.32	-	40.00	20.00	2500.00
Nitrogen	550.37	2.47	-	35.00	20.00	2500.00
Nitrogen	549.90	3.36	549.37	30.00	20.00	2500.00
Nitrogen	549.56	4.92	539.48	25.00	20.00	2500.00
Nitrogen	549.33	7.64	514.70	20.00	20.00	2500.00
Nitrogen	549.18	13.62	469.95	15.00	20.00	2500.00
Nitrogen	549.08	30.63	392.62	10.00	20.00	2500.00
Projectile according to Level III threat with different diameter sabot (10 g each, 19.6 g total weight)						
Gas	V_{max} (m/s)	Barrel length [m]	V_{3m} [m/s]	Sabot diamter [mm]	Pressure [N/mm²]	Reservoir [cm³]
Helium	872.19	3.15	871.79	40.00	20.00	2500.00
Helium	871.52	4.16	862.35	35.00	20.00	2500.00
Helium	871.04	5.65	836.01	30.00	20.00	2500.00
Helium	870.71	8.14	794.33	25.00	20.00	2500.00
Helium	870.49	12.77	725.36	20.00	20.00	2500.00
Helium	870.34	22.66	625.66	15.00	20.00	2500.00
Helium	870.26	50.98	485.79	10.00	20.00	2500.00
Projectile according to Level III threat with different diameter sabot (10 g each, 19.6 g total weight)						
Gas	V_{max} (m/s)	Barrel length [m]	V_{3m} [m/s]	Sabot diamter [mm]	Pressure [N/mm²]	Reservoir [cm³]
Hyrdogen	1088.17	3.65	1082.25	40.00	20.00	2500.00
Hyrdogen	1087.50	4.88	1060.50	35.00	20.00	2500.00
Hyrdogen	1087.06	6.61	1013.91	30.00	20.00	2500.00
Hyrdogen	1086.79	9.46	949.99	25.00	20.00	2500.00
Hyrdogen	1086.62	14.73	850.53	20.00	20.00	2500.00
Hyrdogen	1086.54	26.24	715.97	15.00	20.00	2500.00
Hyrdogen	1086.50	58.92	535.31	10.00	20.00	2500.00

I. PRESSURE RESERVOIR AND GAS SOURCE

In order to keep the design as simple and also as cheap as possible, it is intended to utilize a gas source of a size that it can serve directly as pressure reservoir as well. A simply and safe solution for that would be a gas bottle of the required reservoir size. This size of gas bottle is utilized for example in sports diving as a “pony bottle”, a secondary cylinder as a backup system if the diver or an accompanying diver should suffer lack of oxygen due to either technical failure or human mistake.

Figure 3: Primary and "pony" gas bottle for diving (12 l and 3 l); Source: http://en.wikipedia.org/wiki/File:12_and_3_litre_diving_cylinders.JPG

Figure 3 shows a pony bottle and a primary cylinder as they are used in diving. This specific pony bottle has a capacity of 3 l, they can be found in various sizes depending on manufacturer. One example for a product overview from Catalina Cylinders is presented by XSScuba at http://www.xsscuba.com/downloads/cylinder_specs/catalina.pdf. In this product range the 2.7 l Catalina S19 should serve nicely as a reservoir, slightly exceeding the 2.5 l that were the basis for Table 1's calculations. Without the usage of sabots therefore maintaining a small bore diameter even the smaller version of 0.9 l should support enough gas to accelerate a projectile close to the values presented in Table 2.

Table 2: Achievable muzzle velocities without sabot and with 1 l gas reservoir

Projectile according to Level III threat (7.62 mm diameter; 9.6 g weight)						
Gas	V_{max} (m/s)	Barrel length [m]	V_{3m} [m/s]	V_{6m} [m/s]	Pressure [N/mm²]	Reservoir [cm³]
Nitrogen	527.99	29.88	378.51	442.19	20.00	1000.00
Helium	849.71	40.52	511.96	631.83	20.00	1000.00
Hydrogen	1054.78	46.74	571.28	725.14	20.00	1000.00

II. TRIGGER MECHANISM AND PROJECTILE HOUSING

Possible trigger mechanisms include rapid opening valves as magnetic valves or simply a diaphragm. Such a diaphragm has been applied successfully by Hutchins and Winter (1974) in the form of a thin copper foil. The thickness has to be calculated so that the foil breaks at the desired pressure, in this case 20 MPa. In order to keep the design as simple as possible, the projectile con simply be inserted into the beginning of the barrel, and the copper foil as trigger mechanism be inserted into the connection between gas reservoir and barrel, which would be the barrel threaded into a slightly larger pressure pipe or hose attached to the cylinder. It should be noted that the strength with which the parts are threaded together has to be controlled or it might damage the copper foil leading to faster failure than anticipated.

III. BARREL

The barrel is to consist of a pipe, which has to be able to withstand higher pressure, for safety reasons it should be able to safely withstand the operating pressure of 20 MPa. Additionally it has to be with very low tolerances regarding diameter and level to ensure that the projectile travels down the barrel without colliding with the barrel walls. It should be mounted on a series of supporting parts, a common way is the displayed y-formed holder.

The entire system up to this point can be mounted on a car, which provides two advantages: It improves the storage of the equipment by enabling the user to drive it into a corner or other area and the recoil will be partly absorbed by driving the entire (heavy) car backwards which will increase the stability and decrease the forces and strains on the system.

IV. TARGET BOX

The target box consists of a device to implant and hold the specimen such as a clamp or a frame. It is important that the holding does not interfere with the sample's defeating mechanism. Around it is important to install hard walls able to defeat projectile particles and splitters from the sample. Also, to furthermore evaluate the experiments it is suggested to implant an optical sensor to measure the projectile velocity and a high speed camera to examine the impact situation in detail. Obviously, the camera would need a bullet-proof transparent housing to protect it.

V. PROJECTILE AND SABOT

The applied projectiles should be chosen according to the NIJ classification of the desired test. The values are shown in Table 3.

Table 2: NIJ Classification

NIJ BODY ARMOR CLASSIFICATION / KINETIC ENERGY				
Type	**Test calibre**	**Mass [g]**	**Velocity [m/s]**	**Energy [J]**
Type IIA	9 mm FMJ RN	8	373	557
	.40 S&W FMJ	11.7	352	725
Type II	9 mm FMJ RN	8	398	634
	.357 Magnum JSP	10.2	436	969
Type IIIA	.357 SIG FMJ FN	8.1	448	813
	.44 Magnum SJHP	15.6	436	1483
Type III	7.62 mm FMJ (M80)	9.6	847	3444
Type IV	.30 AP (M2 AP)	10.8	878	4163

The sabot plays an important role on the flight behavior and performance. The material of choice would be a hard light-weight Polymer. Which material and which geometry would supply the best results have yet to be determined.